Evaluating Holocene natural hazards in the French Massif Central from a regional lake sediment approach

Emmanuel Chapron, Anthony Foucher, Léo Chassiot, W Fleurdeus, V Arricau, Laurent Perdereaux, Isabelle Gay-Ovejero, Marlène Lavrieux, Mikael Motelica-Heino, S Salvador-Blanes

Evaluating Holocene natural hazards in the French Massif Central from a regional lake sediment approach

Emmanuel Chapron, A Foucher, L Chassiot, W Fleurdeus, V Arricau, L Perdereaux, I Gay-Ovejero, M Lavrieux, M Motellica-Heino, S Salvador-Blanes

Evaluating Holocene natural hazards in the French Massif Central from a regional lake sediment approach

E. Chapron [a, *], A. Foucher [b, 1], L. Chassiot [c, d], W. Fleurdeus [a], V. Arricau [a], L. Perdereaux [c], I. Gay-Ovejero [b], M. Lavrieux [c, e], M. Motellica-Heino [c], S. Salvador-Blanes [b]

[a] University Toulouse 2 Jean Jaurès, UMR CNRS 5602 GEODE, 5 Allée A. Machado, 31058, Toulouse Cedex, France
[b] University of Tours, EA CNRS 6293 GéHCO Parc de Grandmont, 37200, Tours, France
[c] University of Orléans, UMR CNRS-BRGM 7327 ISTO1A Rue de La Férollerie, 45071, Orléans Cedex 2, France
[d] [d] Laval University, Geography Department, Pavillon Abitibi-Price, 2405 Rue de La Terrasse, Québec, QC, G1V 0A6, Canada
[e] University of Basel Environmental Geosciences, Bernoullistr. 30, CH-4056, Basel, Switzerland

ARTICLE INFO

Keywords:
Lacustrine sediments
Landslides
Floods
Earthquakes
Holocene
Modern times

ABSTRACT

Geophysical surveys in the Lakes Tazenat, Aydat, Chambon and Lacassou combined with a multiproxy study of sediment cores highlight Late Holocene abrupt environmental changes in the northern part of the French Massif Central (FMC). Dating landslide-induced dust layers and subaqueous slope failures impacting lake basin sedimentary fills suggest regional triggering by palaeo-earthquakes (cluster of events) either in the Puy-de-Sancy volcano area, or along the regional Limagne fault. In the present study, a cluster of palaeo-earthquakes occurring in the Sancy area between AD 1243 and 1270 are documented in the Lakes Montcineyre, Chauvet, Pavin and Guéry, as well as by the formation of Lake Lacassou following the last emplacement of the Dent du Marais landslide in the Chaudefour glacial valley around AD 1250 ± 30. Former cluster of earthquakes occurring near the Limagne fault between AD 580 and 650 are evidenced in Lake Tazenat and in maar Lake Pavin. Lake Pavin present lake-level was similarly favoured by the cluster of earthquakes between AD1243 and 1270 and the occurrence of a slump and an outburst flood event resulting in the bypassing of a palaeo-outlet. Holocene earthquakes near the Limagne fault are suggested in maar Lake Tazenat by coeval mass wasting deposits (MWDs) around 2250 ± 50 cal. BP and around 2730 ± 30 cal. BP. A landslide-induced dust layer dated between 2760 and 2520 cal. BP at the transition from paludal to lacustrine deposits in the Chaudefour glacial valley is suggesting that the formation of Lake Chambon resulted from a first emplacement of the Dent du Marais landslide. Radionuclides and radiocarbon dating in Lake Tazenat suggest variable sedimentation rates over the last millennia due to: (i) floods during the Little Ice Age, (ii) coeval MWDs at the basin edges and an erosive turbidite in the central basin between AD 575 and 625 and (iii) lake eutrophication since AD 1945. More gravity cores are needed to directly sample and date the youngest generation of coeval MWDs detected on seismic profiles in order to test the impact in this lake of the cluster of major historical earthquakes in the FMC between AD 1450 and 1490 near the Limagne fault.

1. Introduction

Lake sediments are key natural archives to track Holocene environmental changes associated with climate variability, human impact and natural hazards (Magny et al., 2013; Normandeau et al., 2013; Strasser et al., 2013; Wirth et al., 2013; Gomez et al., 2015; Ross et al., 2015; Van Daele et al., 2015; Arnaud et al., 2016; Chassiot et al., 2018). Natural hazards such as floods, earthquakes, landslides and volcanic eruptions, are developing specific event layers that can be distinguished from regular "background" sedimentation and precisely dated in lacustrine basin fills, when combining high-resolution geophysical surveys (sub-bottom hydro-acoustic profiles and bathymetry) and multi-proxy studies of well-dated sediment cores and historical data (Chapron et al., 1999, 2007, 2016b, 2007; Lauterbach et al., 2012; Simonneau et al., 2013b; Kremer et al., 2015; Hansen et al., 2016; Knapp et al., 2017 Labuhn et al., 2018; Rapuc et al., 2018). Comparatively to lacustrine

* Corresponding author.
E-mail address: emmanuel.chapron@univ-tlse2.fr (E. Chapron).
[1] Present address: University Paris-Saclay, UMR CNRS-CEA 8212 LSCE Orme Des Merisiers, 91191, Gif-sur-Yvette Cedex, France

https://doi.org/10.1016/j.quaint.2021.05.018
Received 20 December 2018; Received in revised form 14 May 2021; Accepted 16 May 2021

deposits, mire (or paludal) deposits are formed under limited and variable water depths or are only periodically inundated. Paludal deposits may thus not provide continuous sedimentary sequences over long time periods. When complete and well-dated, a stratigraphic sequence of mire deposits can, however, provide valuable records of abrupt, brief and catastrophic events bringing absolute markers of regional significance such as tephra layers (volcanic ash-falls), in situ earthquake-induced liquefaction features (seismites) and flood deposits (Vernet, 2013). One of the commonly documented seismites in stratified sedimentary environments including sandy layers are in particular ball-and-pillow structures (Sims, 2012). Peat deposits frequently developed in regions bearing lakes and mires of glacial or volcanic origins, are in addition, important natural archives to establish a regional tephrostratigraphy (Juvigné and Miallier, 2016; Jouannic et al., 2014) and to better understand the evolution of human activities on environmental changes (Miras et al., 2004).

Co-seismic subaqueous and/or subaerial slope failures associated with earthquakes are among the most dangerous natural hazards and are widespread phenomena within tectonically active mountain ranges (Chapron et al., 2007; Howarth et al., 2013; Nepop and Agatova, 2016; Knapp et al., 2017). Although infrequent, large earthquakes are thus important drivers of topographic developments in mountain landscapes (Densmore et al., 2009). Co-seismic landsliding are also increasing hillslope susceptibility to failure during subsequent storms (Hovius et al., 2011; Howarth et al., 2013). Observations on landscape responses following historic earthquakes and subaerial slope failures highlight that increased rates of erosion can persist for years to decades, making earthquakes important contributors to long-term erosion rates (Densmore et al., 2009; Howarth et al., 2013).

The main stratigraphic signature of earthquakes in mountainous environments consist in (i) coeval subaquatic mass-wasting deposits (MWDs) developed at a regional scale in different lake basins (and/or within lake sub-basins) identified either in shallow or deep water environments (Chapron et al., 2007, 2012, 2016b; Strasser et al., 2013; Simonneau et al., 2013b; Van Daele et al., 2015; Oswald et al., 2021); (ii) subaerial landslides or rockfalls deposits near active faults and/or within glacial valleys (Schneider et al., 2004; Deplazes et al., 2007; Howarth et al., 2013; Nepop and Agatova, 2016; Knapp et al., 2017) and (iii) in-situ liquefaction features within generally shallow water environments (lakes or mires) and in between recent sedimentary layers with contrasted grain size (Beck et al., 1996; Beck, 2009; Sims, 2012).

The sensitivity of lake systems to earthquakes can be expressed as a combination of external factors (earthquake magnitude, lake-epicentre distance and regional geological context) and internal factors (lake morphology, nature of sediment, sedimentation modes, lake-level fluctuations and changes in sedimentary load). Lake sensitivity to earthquake-induced slope failures may thus not be absolutely stable over long periods, but varying with changes in sedimentation modes resulting from climate changes during the Holocene (Chapron et al., 2016b). In the French Massif Central (FMC), historical human-induced changes in catchment erosion have in addition enhanced sedimentary load in lakes since the onset of the Little Ice Age (LIA), which increased lake sensitivities to earthquake ground shaking (Chassiot et al., 2016b; This Issue).

The aim of this study presenting unpublished data from the Lakes Aydat, Chambon, Lacassou (linked to Lake Chambon formation) and Tazenat (Fig. 1) is to document dominating sedimentary processes in these small lakes from the FMC and to determine the age, impact and origin of slope failure events. A compilation of these new data with former studies in surrounding lakes (Pavin, Chauvet, Guéry and Montcineyre) and in the nearby Limagne mire (Fig. 1) is finally presented in order to better evaluate the exposure of the FMC to natural hazards, with a focus on earthquakes.

2. Regional setting

2.1. French Massif Central specificities

The FMC is a mid-latitude and mid-altitude mountainous area hosting a succession of volcanic edifices (Fig. 1). To the North, the Chaîne-

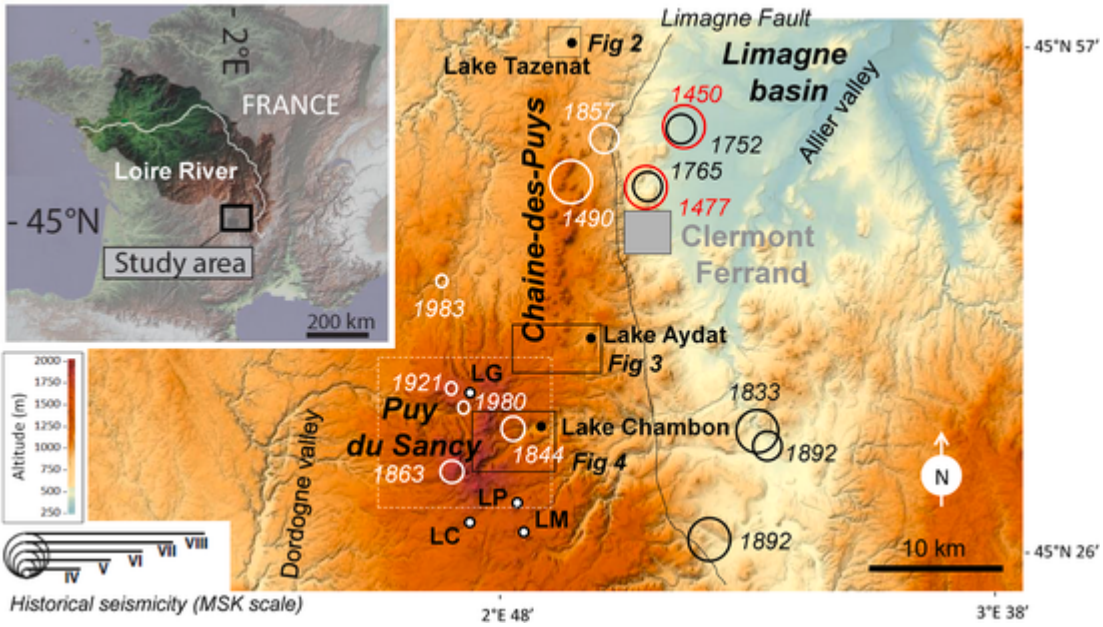

Fig. 1. General location of the study area and French Massif Central (FMC) within the drainage basin of the Loire River (upper left) and location of historical earthquakes and studied lakes (black dots are lakes presented in this paper and white dots are previously studied lakes discussed in this paper; Lake Abbreviations: LC: Lake Chauvet, LM: Lake Montcineyre, LG: Lake Guéry, LP: Lake Pavin). The city of Clermont-Ferrand in the Limagne basin is located east from the Chaîne des Puys volcanic province of Holocene Age and next to the active Limagne fault (black line). Lake Tazenat is a maar lake (such as LP and LC), while Lake Aydat is dammed by a lava flow and Lake Chambon is dammed by the largest known landslide of the FMC. Except LC and LG none of the other studied lakes were covered by glaciers during the last glaciation. The white rectangle is locating the Mont Dore volcanic province culminating with the Puy-du-Sancy volcano. Abbreviation MSK = Medvedew-Sponheuer-Karnik.

des-Puys culminating at 1465 m above sea level (a.s.l.) is a volcanic province (formed between ca. 70 kyrs before present (BP) and 8550 ± 400 cal. BP) separated from the Limagne graben by the Limagne Fault, a major and active normal fault (Boivin et al., 2009). To the South, the Puy-de-Sancy stratovolcano (1886 m a.s.l.) was formed during the Pleistocene and constitutes the youngest volcano of the Mont Dore massif. The flanks of this stratovolcano were shaped by mountain glaciers extending down to ca. 650 m a.s.l. during the last glacial period (Etlicher and de Goër de Herve, 1988; Defive et al., 2019). Four small nearby volcanoes developed along the southern flanks of the Puy-de-Sancy during the Early Holocene within a short period completed ca. 7000 years ago by the violent phreatomagmatic eruption that formed maar Lake Pavin (see Chapron et al. (2012) and Juvigné and Miallier (2016) for a review). The study area is characterized by numerous small lakes with contrasted setting and morphologies (Juvigné and Stach-Czerniak, 1998; Gay and Macaire, 1999; Chapron et al., 2012; Lavrieux et al., 2013a; Chassiot et al., 2016b) formed after glacier melting (e.g. Lake Guéry), a phreatomagmatic eruption (e.g. the maar Lakes Tazenat, Chauvet and Pavin) or dammed either by a lava flow (e.g. Lake Aydat), the edification of a stratovolcano (e.g. Lake Montcineyre, palaeo-lake Tartaret) or by a landslide (e.g. Lake Chambon). Today, the seismic hazard in the study area is considered as moderate (Fig. 1). The reported earthquakes for the last 500 years were essentially clustered along the Limagne fault and beneath the Mont Dore massif (see Chassiot et al., 2016b for a review). Human-induced landscape openings inferred from palynological. studies were initiated during the Neolithic period, and rose until a significant demographic decline during the late 19th century (Miras et al., 2004, 2015; Lavrieux et al., 2013a; Chassiot et al., 2018, Chassiot et al., This Issue). Climate change and land use during the LIA also favoured enhanced flooding events, soil erosion and lacustrine sedimentation. Today, economically the study area relies on industrial activities around the city of Clermont-Ferrand in the Limagne basin, as well as on tourism and agriculture in mid–elevation mountain landscapes (< 1500 m a.s.l.). Climatic conditions and precipitation patterns ranging from 1200 to 1600 mm.yr^{-1} are mainly related to the influence of Atlantic westerlies and frequently favor snow falls during winters in this territory (Stebich et al., 2005; Chassiot et al., 2018).

2.2. Lake Tazenat settings

Lake Tazenat is the northernmost maar from the Chaîne-des-Puys and was formed within crystalline Palaeozoic rocks during the early Late-Glacial period between 29 and 34 kyrs (Valentine et al., 2019). This mesotrophic lake, located at an elevation of 633 m a.s.l., has a bowl shape morphology with a diameter of about 700 m covering an area of 0.6 km^2 (Fig. 2) with a maximum water depth of 67 m (Delebecque, 1898). Lake Tazenat is surrounded by a marked crater rim and supplied by temporary springs rising around its shore and by the Rochegude stream that is deeply incised in the topography (up to 12 m incision) and developing a small delta to the south of the lake (Juvigné and Stach-Czerniak, 1998). This stream is following the Rochegude fault, a small NNE-SSW fault parallel to regional major joints (cf. Fig. 2) linked to the Limagne fault system (Valentine et al., 2019). Springs and stream bringing water to Lake Tazenat are influenced by regional faults and the hydrological drainage basin of the lake is thus probably larger than the topographic drainage basin. As shown in Fig. 2, the Rochegude stream is incised within an elongated drainage basin (2.66 km^2) culminating at 753 m a.s.l along northern slopes of the Puy Chalard scoria cone (Juvigné and Stach-Czerniak, 1998; Valentine et al., 2019). The topographic catchment is characterized by up to 1 m thick gleyed soils

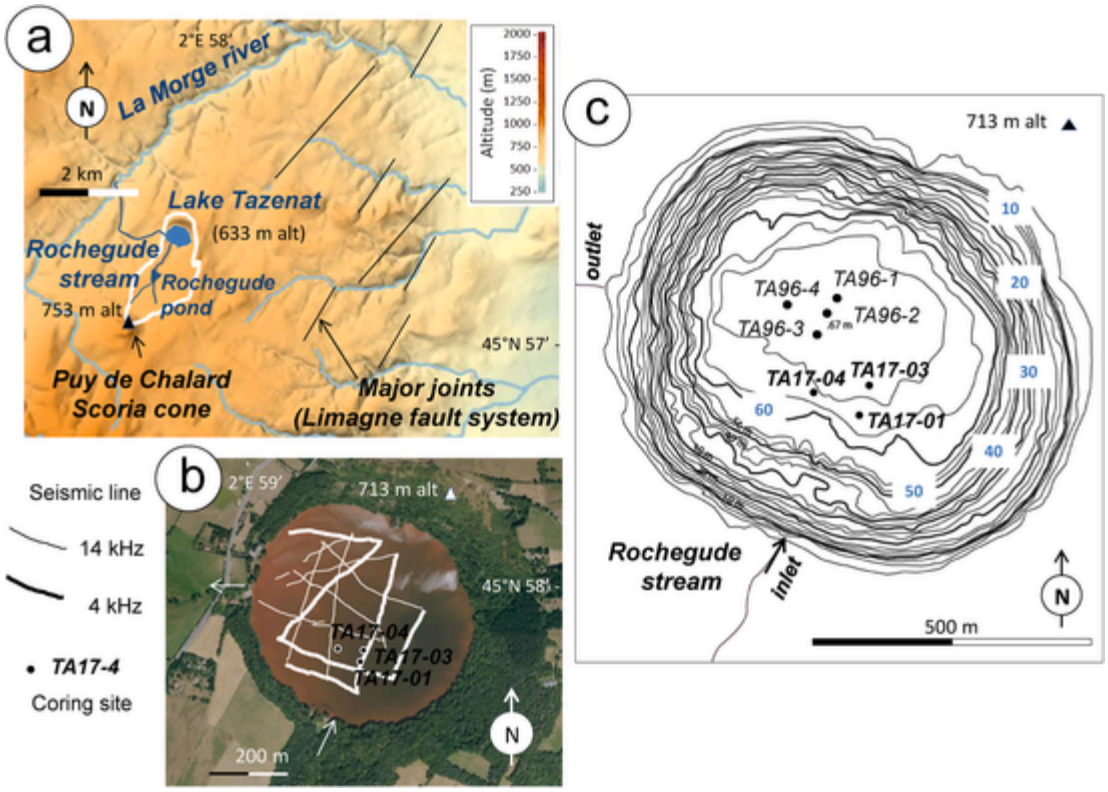

Fig. 2. General settings of the maar lake Tazenat in the FMC, and available environmental data: (a) location of the Lake Tazenat drainage basin (white line), Rochegude stream (blue line) and Rochegude pond discussed in the text; (b) location of seismic profiles (14 or 4 kHz) collected in 2017 to optimize the coordinates of new gravity cores, note the red color of the lake waters during summer 2016 due to an exceptional cyanobacteria bloom; (c) Bathymetry of Lake Tazenat (isobaths: 3 m) combining manual measurements from Delebecque (1898) along the steep slopes of the maar and continuous echo sounding measurements (200 kHz) acquired together with seismic profiles in 2017 in the deep basin. Also indicated are the location of long piston cores collected in 1996 and detailed by Juvigné and Stach-Czerniak (1998). (For interpretation of the references to colour in this figure legend, the reader is referred to the Web version of this article.)

covered by meadows, wooded areas and the Rochegude pond (De Crespin de Billy et al., 2000) formed after AD 1866, according to old regional topographic maps). The lake outlet flows on gentles slopes towards the West first into a small peat bog and an artificial pond (already indicated on AD 1866 maps) and then into the Morge River, a tributary of the Allier River (one of the main mountainous tributary of the Loire River, Fig. 1). Palynological. and sedimentological investigations by Juvigné and Stach-Czerniak (1998) of a 10 m long core taken in the muddy deposits of the flat bottom of Lake Tazenat (Fig. 2) revealed: (i) the persistence of a dense forest since the early Late-Glacial, before phases of human deforestation by Neolithic, Celtic and subsequent populations; (ii) three tephra beds at 875 cm, 783 cm and 675 cm below lake floor (b.l.f.), respectively (the last one being linked to the Pavin volcano) and (iii) three striking sandy layers interbedded (at 87 cm, 263 cm and 277 cm b.l.f., respectively) in Subboreal to Subatlantic mud. Recent sediments in Lake Tazenat are in addition characterized by C/N ratio <10 (Mallet et al., 2006) typical for algal organic matter (Meyers, 1994). As shown in Fig. 2b, Lake Tazenat waters turned red during summer 2016 due to an exceptional bloom of cyanobacteria.

2.3. Lake Aydat settings

Lake Aydat is located at the southern boundary of the Chaîne-des-Puys volcanic range and East of the Puy-de-Sancy stratovolcano (Figs. 1 and 3) on a plutonic and metamorphic substratum partly covered by Late-Glacial to Holocene volcanic deposits. This eutrophic lake originates from the damming of the Veyre River by a basalt flow issued from the last eruption of the Puy de la Vache and Puy de Lassolas volcanoes dated to 8550 ± 400 cal. BP (Boivin et al., 2009). As detailed in Lavrieux et al. (2011, 2013a), Lake Aydat has a maximum water depth of 15 m, a surface of 0.6 km^2 and is draining an elongated catchment area of 30 km^2 characterized by grasslands, pastures and secondary forests developed on quite shallow andosols (<30 cm). A multidisciplinary study of a 19 m long core (AYD09) taken in the flat bottom of the lake (Fig. 3) did not reach the bedrock but revealed contrasted sedimentary units deposited over the last 6700 years (Lavrieux et al., 2013a): a lower unit (Mid Holocene) displaying a fine and regular lamination is capped by a pluri-metric (and erosive) MWD triggered ca. 1780 ± 40 cal. BP, while the upper unit (Late Holocene) is made of organic rich and fine-grained, faintly laminated sediments with numerous interbedded flood deposits and diatom blooms. Identified flood events and phases of eutrophication during the Late Holocene were related to increasing anthropogenic pressure (deforestation, pastures, hemp cultivation and retting) according to Lavrieux et al. (2013a, b).

2.4. Lake Chambon and Lake Lacassou settings

The Lake Chambon catchment (in the Chaudefour valley) culminating at 1883 m a.s.l. is located on the eastern flank of the Puy-de-Sancy stratovolcano (Fig. 4). The Chaudefour valley is a glaciated valley made of granites and metamorphic rocks covered mainly by Mio-Plio-Quaternary basalts and trachyandesites, glacial tills, fallen debris material (originating from the collapse of steep slope rocks) and Late-Glacial to Holocene fluvial and lacustrine sediments (Dupuis et al., 1996; Vidal et al., 1996; Macaire et al., 1997; Gay and Macaire, 1999). Three lakes formed successively in the Chaudefour valley (Fig. 4): (i) the Tartaret palaeo-lake was formed after the damming of the Chaudefour River by the Tartaret stratovolcano ca. 15000 cal. BP, and a lake remained at an elevation of 890 m a.s.l. until ca. 9800 BP (ca. 11000 cal. BP), then drained probably totally around ca. 9500 cal. BP, and developed flu-

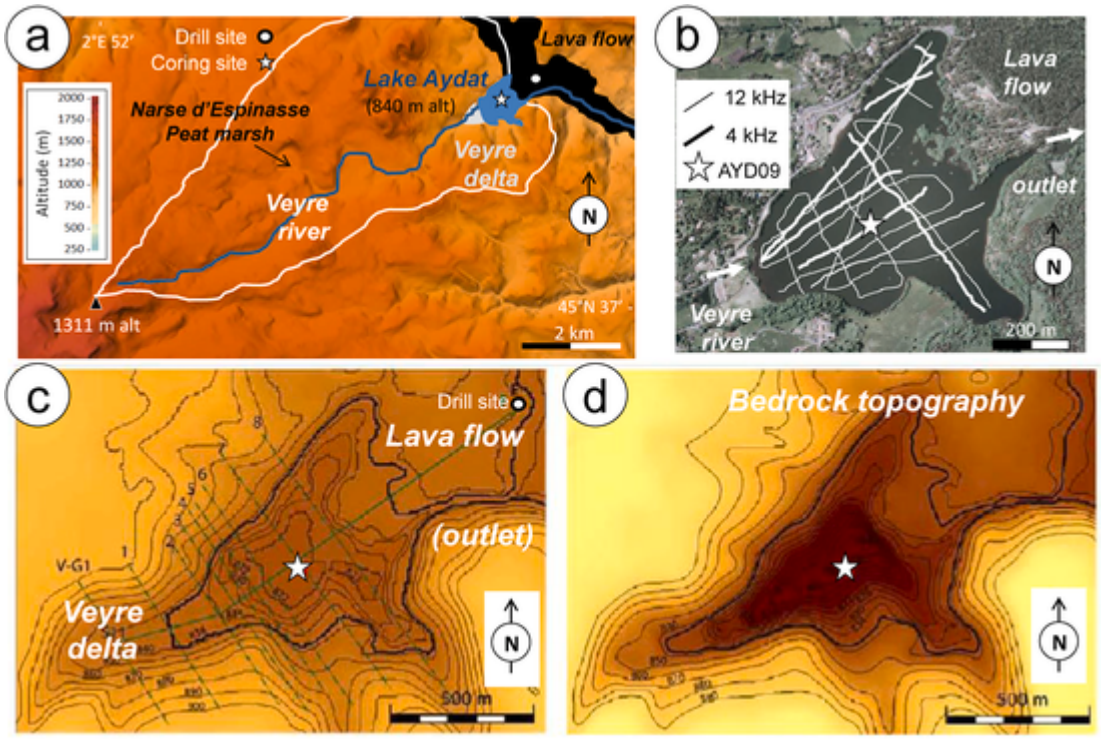

Fig. 3. General settings of Lake Aydat in the FMC, and available environmental data: (a) location of the Lake Aydat drainage basin (white line), Veyre River (blue line), Veyre delta (grey triangle), the lava flow (black colour) that formed the lake, the Narse d'Espinasse peat marsh and the drill (white spots) and coring sites (white stars) discussed in the text; (b) satellite image of Lake Aydat together with seismic lines (12 and 4 kHz) and AYD09 long piston coring site (white star) (c) geomorphological context of Lake Aydat integrating its surrounding topography (isoline 10 m) and lake bathymetry (isobaths 4 m transformed in isolines of altitude above sea level) together with the location of the drill site (white dot), the AYD09 coring site (white star) and topographic transects allowing to estimate the basement slopes surrounding the lake and the thickness of the sedimentary infill of the lake as discussed in the text; (d) Lake Aydat bedrock topography deduced from the extrapolation of basement slopes below the lake and the Veyre delta and from bedrock altitude measured at the base of the lava flow drill site as detailed in the text. (For interpretation of the references to colour in this figure legend, the reader is referred to the Web version of this article.)

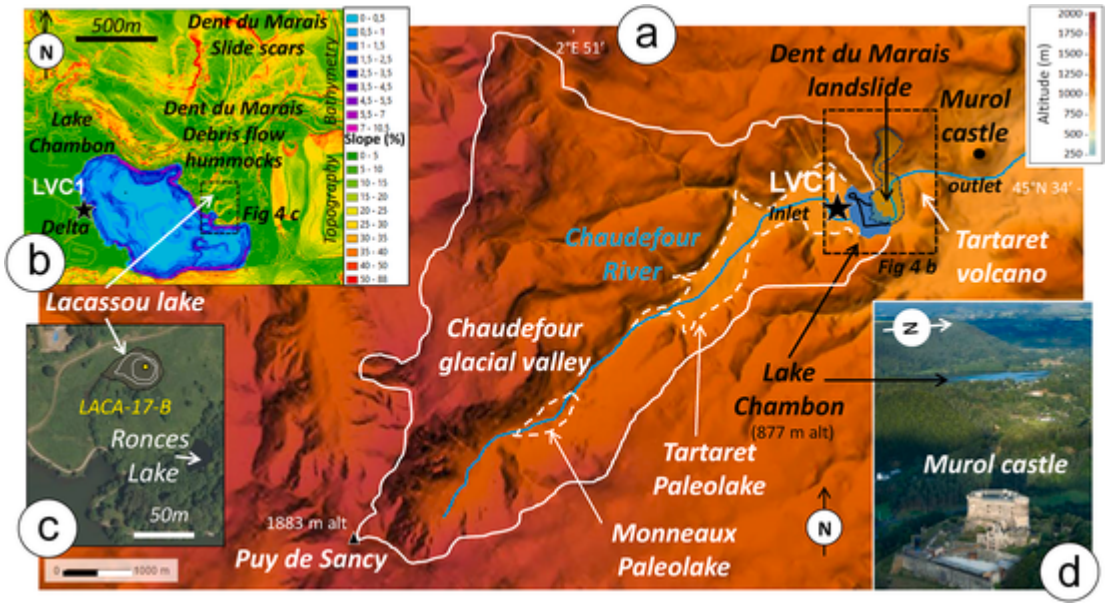

Fig. 4. General settings of Lake Chambon in the FMC, and available environmental data: (a) location of the Lake Chambon drainage basin (white line), Chaudefour River (blue line), Tartaret and Monneaux palaeo-lakes (white dotted lines), Dent du Marais landslide (black dotted line), Tartaret volcano, LVC1 drill site (black star) from the Chambon system (detailed in Macaire et al., 1997), Lake Chambon 14 kHz seismic profiles (black lines), and the Murol castle (black spot) discussed in the text; (b) topographic slope map of the Lake Chambon area showing the Dent du Marais landslide units, the Lake Chambon bathymetry in 2009, and the location of Lake Lacassou; (c) satellite image of Lake Lacassou, with 1 m isobaths from 2017 and the location of core LACA-17-B and Lake Ronces discussed in the text; (d) aerial picture from the Murol castle, with Lake Chambon in the Chaudefour valley in the background (courtesy of Francis Cormon). (For interpretation of the references to colour in this figure legend, the reader is referred to the Web version of this article.)

vial, deltaic and lacustrine deposits (pebbles, sands and silts) reaching a total volume of ca. 11 × 10^6 m^3, (ii) the Monneaux palaeo-lake formed around 9500 cal. BP by the emplacement of the Plate rock fall which blocked the upper valley and was quickly filled by laminated lacustrine sediments and (iii) the present Lake Chambon was formed after the damming of the valley by the Dent du Marais landslide after ca. 2700 cal. BP. According to Vidal et al. (1996), the Dent du Marais landslide (Fig. 4b) is the largest known landslide of the FMC and is characterized by 90 m high slide scars within Mont Dore volcanoclastic products of Pliocene age covering a formation of Oligocene age made of clays and gravels. The associated deposits (ca. 7 × 10^6 m^3 according to Macaire et al., 1992) are evolving down slope into a debris avalanche over a distance of 1600 m and developing a hummocky topography that created Lake Chambon but also two very small lakes (Lacassou and Ronces lakes, Fig. 4b and c and). Lake Lacassou was nucleated in a small topographic depression on the debris avalanche deposits (made of metric to plurimetric blocs and megablocs imbedded within a fine grained matrix) and gave birth to an outlet that ends quickly in Lake Chambon (Fig. 4c). Lake Ronces is in a similar setting but this small basin is not connected to Lake Chambon. The outlet of Lake Chambon runs over the landslide deposits and the lake-level is today artificially regulated. A bathymetric map of Lake Chambon realized in March 2009 for an environmental state agency clearly revealed that this lake is now very shallow (maximum 3 m deep) and that the debris avalanche deposits are extending below the lake surface (877 m a.s.l.) along its eastern shore. As shown by a slope map of the Dent du Marais landslide (from a DEM with 1 m resolution) and Lake Chambon bathymetry (Fig. 4b), this lake is strongly influenced by the landslide. The western shore of the lake is less steep and resulted from the progradation of the Chaudefour River delta that was drilled and mapped on land as detailed in Gay (1995), Dupuis et al. (1996) and Macaire et al. (1992, 1997). The LVC1 drill site located next to the lake shore (Fig. 4) revealed, in particular, that the granitic bedrock is here at 20 m depth and capped by tills, lacustrine and deltaic deposits (silty clays and sandy gravels) linked to the Tartaret palaeo-lake, a ca. 1 m thick paludal sequence, and another sequence of silty clays and sandy gravels resulting from the progradation of the Chaudefour River delta in Lake Chambon.

3. Materials and methods

A multidisciplinary limnogeological approach of the Lakes Tazenat, Aydat, Chambon and Lacassou was recently realized to regionally extend the characterization of lacustrine sedimentation performed in Lakes Pavin, Chauvet, Montcineyre, Guéry (Chapron et al., 2010, 2012, 2016a; Chassiot et al., 2016b, b; 2018) and Aydat (Lavrieux et al., 2013a).

3.1. Sub-bottom acoustic profiling

A portable Knudsen bi-frequency sub-bottom profiler (Pinger system) including a 200 kHz echosounder transducer and two interchangeable (4 or 14 kHz) pinger sources used with a modulating frequency (CHIRP) and a large aperture hydrophone receive array was used from an inflatable boat on the Lakes Tazenat, Aydat and Chambon to map the lake bathymetry and basin fill geometry. A conventional GPS connected to an external digital data logger through a PC was used to digitalize the acoustic data and to generate grids of sub-bottom profiles (Figs. 5 and 6). Acoustic data (SEG-Y format) were then examined using open source SeiSee software. EDIFISegY software (Chapron, 2016) was used to map key reflections and export them in shapefile format into a GIS to produce bathymetric maps. For Lake Tazenat, isobaths from the bathymetric map of Delebecque (1898) were in addition digitalized and combined into a GIS with lake bathymetric measurements realized during the 2017 summer survey (Fig. 2). For Lake Lacassou, a Garmin GPS echosounder (200 kHz) was used from an inflatable boat to record bathymetric transects (Fig. 4c).

3.2. Sediment coring

Three short gravity cores (Figs. 2, 7 and 8) were retrieved in Lake Tazenat (TA17-01, −03 and −04) in June 2017 with an UWITEC corer

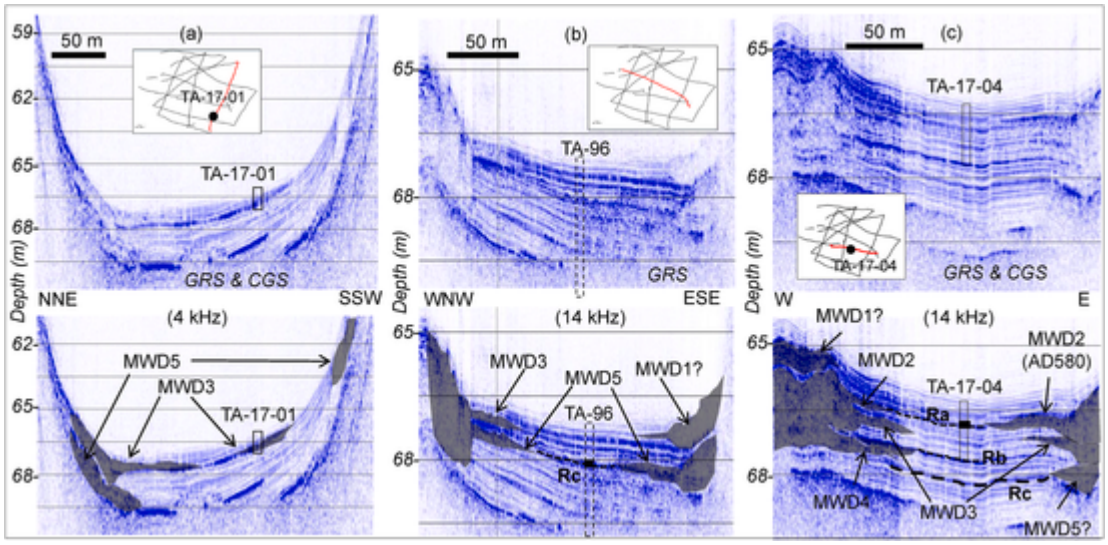

Fig. 5. Selected seismic profiles from the Lake Tazenat in the FMC (a,b,c), highlighting lake floor morphologies and basin fill geometries when gas rich sediments (GRS) are not preventing the penetration of the acoustic signal. The locations of sediment cores discussed in the text are indicated and allow calibrating acoustic facies. Black bars in cores TA-96 and TA-17-04 are coarse sand layers discussed in the text. Mass wasting deposits (MWD) are identified by lens-shaped bodies (grey lenses).

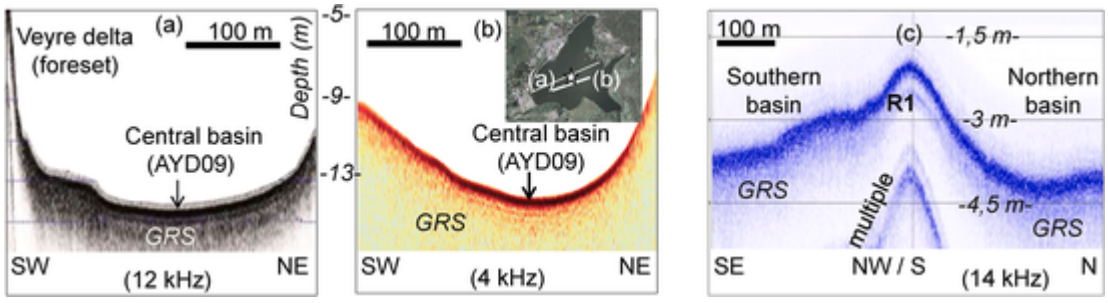

Fig. 6. Selected seismic profiles from Lake Aydat (a,b) and Lake Chambon (c) in the FMC, highlighting lake floor morphologies, but no basin fill geometries where gas rich sediments (GRS) are preventing the penetration of the acoustic signal. The locations of sediment cores discussed in the text are indicated.

from two coring sites. As shown in Figs. 2 and 6, the new coring locations were selected in the central basin, but closer to the delta than former piston-coreTA-96 studied by Juvigné and Stach-Czerniak (1998). The core AYD09 (Fig. 9) was collected from the central basin of Lake Aydat in 2009 from an UWITEC coring platform with a piston corer as detailed in Lavrieux et al. (2013a). The coring site was here selected based on lake floor geomorphology in the flat central basin (Figs. 3 and 6). In Lake Lacassou, two twin short gravity cores (LACA-17-A and LACA-17-B) were sampled in June 2017 from the central basin (Figs. 4c and 10 and) based on bathymetric measurements.

3.3. Core sedimentology

Sediment cores were split in two halves and their stratigraphy were detailed visually. In cores from the Lakes Tazenat, Aydat and Lacassou, sediment magnetic susceptibility (MS) was measured with a Bartington magnetometer and a MS2E point sensor at every centimetre. In addition, sediment diffuse spectral reflectance measurements were performed every centimetre on cores TA17-01, TA17-04 and LACA-17-B with a Minolta CM-700 d. Color pictures from cores LVC1 and LACA-17-B were used to characterize changes in sedimentation modes (Fig. 10). Lake Aydat cores sections were imaged by a digital camera and MS measurements were realized at high resolution on a GEOTEK core logger (Fig. 9). Bulk sediment organic carbon content and element composition from core AYD09 were estimated by Rock-Eval pyrolysis and a XRF core scanner (Avaatech Core Scanner), respectively, as detailed in Lavrieux et al. (2013a). The sediment geochemistry from core AYD09 was further analysed by Laser Ablation ICP-MS, following procedures described by Gratuze et al. (2001) and Simonneau et al. (2013a). Up to 19 ICP-MS samples from core AYD09 were collected and measured at the IRAMAT laboratory (CNRS Orléans) to calibrate the X-ray fluorescence measurements from the Avaatech core scanner (Fig. 9). This calibration allows obtaining high-resolution values (every centimetre) of TiO_2 and K_2O contents from core AYD09, two classical proxies of terrigenous sediment supply. Grain size analyses were performed every cm on core TA-17-01 and TA-17-04 (Fig. 7) by laser diffraction using a Malvern Mastersizer 3000 The detailed stratigraphy of cores TA-17-01 and TA-17-04 was determined using relative sediment density recorded every 0.6 mm by Computed Tomography images (CT scans) obtained by using facilities (Siemens Somatom 128 Definition AS scanner) of the CIRE platform (Surgery and Imaging for Research and Teaching, INRA Val de Loire). The relative densities (expressed in Grey scale values) from these CT scan data were extracted from the scanner imagery with the free software ImageJ (Schneider et al., 2012; Foucher et al., 2019).

3.4. Core chronology

Seventeen AMS radiocarbon dates distributed over core AYD09 (Fig. 9), based on leaf and wood fragment analyses were obtained at the Laboratoire de Mesure du Carbone 14 (Gif-sur-Yvette, France) and calibrated using CalPal Online (Danzeglocke et al., 2011) as detailed in Lavrieux et al. (2013a). As illustrated in Figs. 7 and 8, the chronology of cores TA-17-04 (three samples) and LACA-17-B (two samples) were similarly based on leaf and wood fragment analyses obtained at the

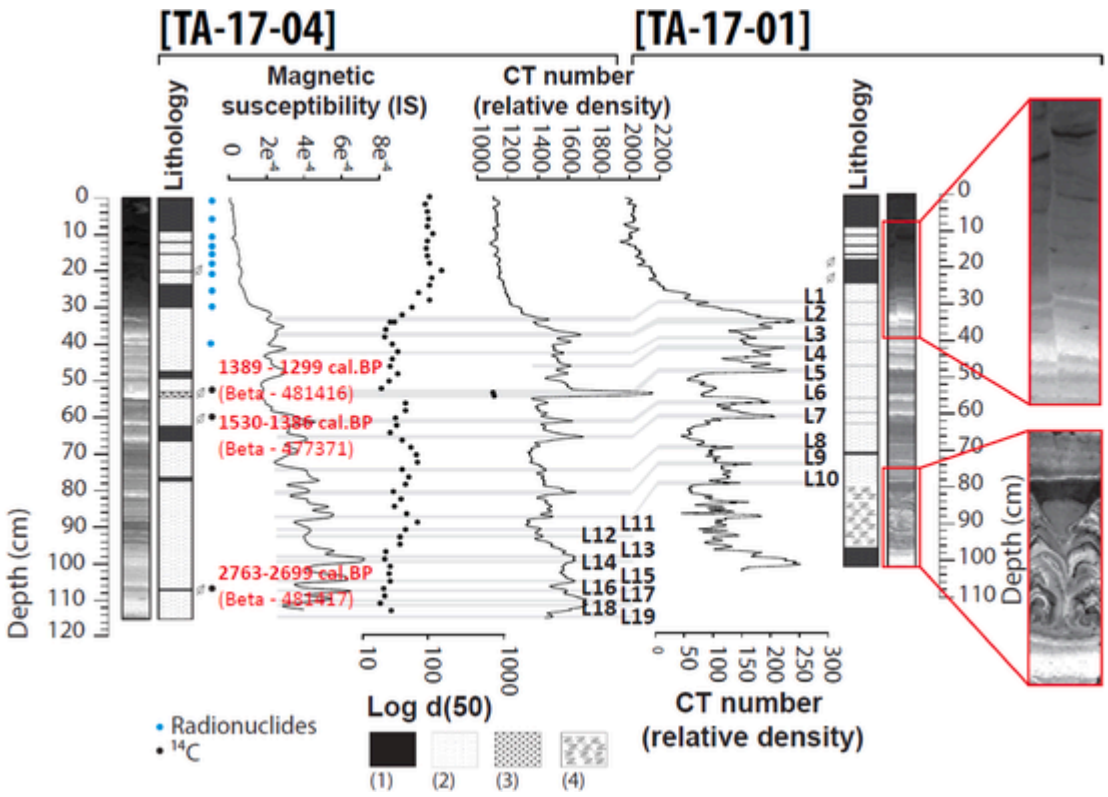

Fig. 7. Lithology and chronology of short gravity cores from the sediments of Lake Tazenat in the FMC. In core TA-17-04 radiocarbon samples (black dots) allow dating sand layers labelled L5, L6 and L16. Measurements of unsupported ^{210}Pb (blue dots) suggest a significant change is sedimentation rate in the upper unit compared to radiocarbon ages from the lower unit. Stratigraphic correlations of event layers (L1 to L10) are based on measurements of sediment magnetic susceptibility (MS), laser grainsize (log D50 in micron meters) and CT scan relative densities in core TA-17-01 allow dating a mass wasting deposit identified on CT scan images just below flood deposit L10. High-amplitude seismic reflection (Ra and Rb) are correlated with sand layers in core TA-17-04. The core lithologies are composed from top to base by: authigenic lacustrine sediment (1); clastic lacustrine sediments rich in flood layers (L1 to L19) (2); sand layers (3) and mass wasting deposit (4). (For interpretation of the references to colour in this figure legend, the reader is referred to the Web version of this article.)

Beta Analytic Radiocarbon Dating Laboratory (Miami, USA) and calibrated using IntCal13 Calibration software (Table 1). Published radiocarbon data from LVC1 core were also calibrated using IntCal13 and included in Table 1.

The chronology of the upper part of the TA17-04 core was also established using excess of Lead-210 ($^{210}Pb_{ex}$) and Caesium-137 (^{137}Cs) activities (Fig. 8) analysed in 10 samples (blue points in Fig. 7) of dried material (~10 g). These gamma spectrometry measurements were obtained with the very low background GeHP detectors available at the Laboratoire des Sciences du Climat (Gif-sur-Yvette, France). Radionuclide activities were decay-corrected to the sampling date and ^{210}Pb ages were determined using the Constant Initial Concentration model (CIC). The $^{210}Pb_{ex}$ age model was validated through the identification of those deposits tagged with peak ^{137}Cs concentrations (Fig. 8). This artificial radionuclide may originate from two sources in Western Europe: thermonuclear weapon testing (maximal emission in 1963) and the Chernobyl accident (1986). To distinguish between both potential ^{137}Cs sources, Americium-241 (^{241}Am), was used to identify the ^{137}Cs peak attributed to the maximum nuclear bomb fallout.

3.5. Quantitative geomorphology

Because gas-rich sediments in Lake Aydat absorbed the entire acoustic signal emitted by the sub-bottom profiler (Fig. 6), it was not possible to image the basin fill geometry. A quantitative geomorphological approach was thus realized to estimate the bedrock topography below the lake and the thickness of its basin fill using GIS (ArcGIS software). A detailed (5 m resolution) digital elevation model (DEM) from the Institut Géographique National (IGN) was first merged with Lake Aydat bathymetric map once isobaths were transformed into isolines of altitude a.s.l. (Fig. 3c). The altitude of the bedrock bellow the lava flow was documented by the description of a drill (Auriat, 1957) located in Fig. 3c. In 2010, fieldwork measurements of the Veyre delta and of the lava flow geomorphologies were also used in order to constrain a spline interpolation of bedrock topographic transects across Lake Aydat area (Fig. 3c). The volume of sediments trapped in Lake Aydat (Fig. 11) was estimated by making the difference in altitude between two layers: (1) the lake floor bathymetry; and (2) the bedrock topography. This latter was obtained after performing a spline interpolation between the altitudes of the bedrock surrounding the lake. All calculations were performed using ArcGIS.

Gas-rich sediments in Lake Chambon similarly prevented imaging the basin fill geometry (Fig. 6). Here a newly available DEM from the IGN with a 1 m resolution was merged with Lake Chambon bathymetric map produced in 2009 and the ArcGIS software was used to generate a slope map of Lake Chambon and the Dent du Marais slide scars and debris flow deposits (Fig. 4b). Field work in winter 2020 allow investigating changes in lacustrine landscapes in the Chaudefour valley during historical time and mapping changes in lake-level and delta geomorphology in Lakes Chambon and Lacassou (Fig. 12).

LIDAR based DEM (20 cm resolution) from Lakes Tazenat and Pavin crater rims were used with ArcGIS software and aerial photographs to document the maar geomorphologies (Fig. 13). Tazenat crater rim slope map was also calculated with ArcGIS and topographic profiles were extracted from the DEM to highlight the morphology of palaeoshorelines (Fig. 13c and d and).

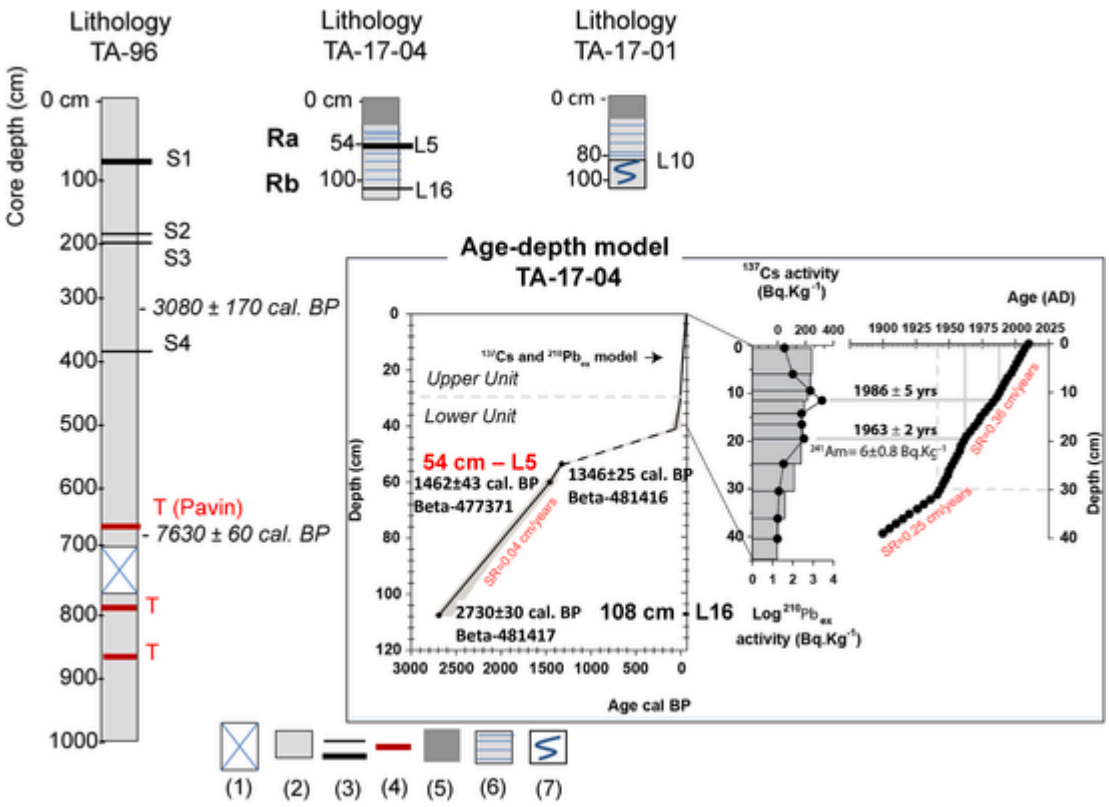

Fig. 8. Synthetic logs of sediment cores extracted from Lake Tazenat in the FMC, and available radiocarbon dates. For core TA-96 key data from Juvigné and Stach-Czerniak (1998) are illustrated: sandy layers (S1 to S4), tephra layers (T) and radiocarbon dates (from bulk sediments) after calibration using the CalPal online program. The age-depth model established for core TA-17-04 (right panel) is based on radiocarbon and radionuclide dates combined with the CLAM software as detailed in the text and on Table 1, and allows dating event layers (L1 to L16) used for the correlation with core TA-17-01. The core lithologies are composed by (1) core gap; (2) organic-rich fine grained lacustrine sediments; (3) sandy layers; (4) tephra layers; (5) upper unit; (6) lower unit; (7) mass wasting deposit.

4. Results

4.1. Lake Tazenat

The bathymetric map of Lake Tazenat (Fig. 2c) illustrates steep slopes down to 57 m water depth surrounding a central basin, excepted in front of the Rochegude river delta, where a step in the morphology is visible between isobaths 33 m and 43 m. Gentle slopes between 57 m and 63 m water depths are, in addition, developing an irregular morphology before reaching a relatively flat central basin of 67 m maximum water depth.

Former higher lake-level are also suggested by LIDAR data in the morphology of the crater rim of Lake Tazenat where three generations of flat palaeo-shorelines are identified on slope maps and topographic profiles (Fig. 13C and d) above the present lake shoreline (located at 630 m above sea level): between 647 and 645 m alt (i.e. 17 to 15 m above the present day lake-level); between 640 and 638 m alt (i.e. 10 to 8 m above modern lake-level) and between 635 and 633 m alt (i.e. 5 to 3 m higher than the modern lake). Lake-level drops are in addition evidenced on LIDAR data by the significant incision both of the lake tributary (ca. 12 m deep) and of the lake outlet (Fig. 13a). Littoral erosion (and/or human impact) following lake-level fall is also locally suggested by the preservation of deltaic environments exposed at the edge of the tributary incised channel (Fig. 13a and b).

A dense grid of sub-bottom seismic profiles (ca. 1800 m of profiles with the 14 kHz source and ca 1200 m with the 4 kHz source, Fig. 2b) clearly imaged the central basin fill geometry down to ca. 3 m b l.f (Fig. 5a, b & 5c). when applying in the sediments a mean P wave velocity of 1500 m/s. Below this depth, the acoustic signal was absorbed in the central basin by gas-rich sediments (GRS). Steep slopes in Lake Tazenat are characterized by a thin to very thin sedimentary cover developing a transparent acoustic facies above the acoustic substratum. At the basin floor periphery and within the basin, lacustrine sediments are developing a seismic facies with high-frequency sub-parallel to divergent continuous reflections of variable amplitudes. Divergent fill geometry is essentially identified along profiles with an N–S orientation, while E-W profiles are illustrating a parallel to sub-parallel seismic facies. Near the basin-floor periphery, numerous mass wasting deposits (MWDs) can be identified on the basis of their transparent-to-chaotic facies smoothly intercalated between continuous reflectors. These lens-shaped bodies are frequently observed at the edges of the basin and can be associated with high-amplitude reflections toward the basin center on 14 kHz profiles (e.g. reflections labelled Ra, Rb and Rc in Fig. 5b and c and). Up to five generations of such MWDs are identified (labelled MWD1 to MWD5 in Fig. 5a, b & 5c) and at least four generations (MWD2 to MWD5) are characterized by stratigraphically contemporaneous MWDs originating from different source areas. These features indicate that multiple sub-lacustrine slope failures occurred at a basin-wide scale. One of these lens-shaped bodies (MWD3) was sampled (Fig. 5a) at the base of core TA-17-01 (100 cm long). In the basin center, high-amplitude reflections labelled Ra and Rb linked with MWD2 and MWD4, respectively, were also sampled in core TA-17-04 (120 cm long). Similarly, reflection Rc associated with MWD5 was probably sampled in core TA-96 (Fig. 5b). Offshore the Rochegude river delta (Fig. 13) and at the location of the morphological step (Fig. 2b), an erosive channel (not shown) is also identified on seismic profiles between ca. 42 m and 59 m water depth.

Two sedimentary units are identified within cores TA-17-01 and TA-17-04 (Fig. 7). An upper unit (0–30 cm core depth in TA-17-04 and 0–28 cm in TA-17-01) is made of dark colored fine grained sediments with low MS (Fig. 7) and low CT-scan relative density values. A lower unit is made of greyish fine grained sediments with higher and variable MS and CT-scan relative density values. Four dark layers in TA-17-04

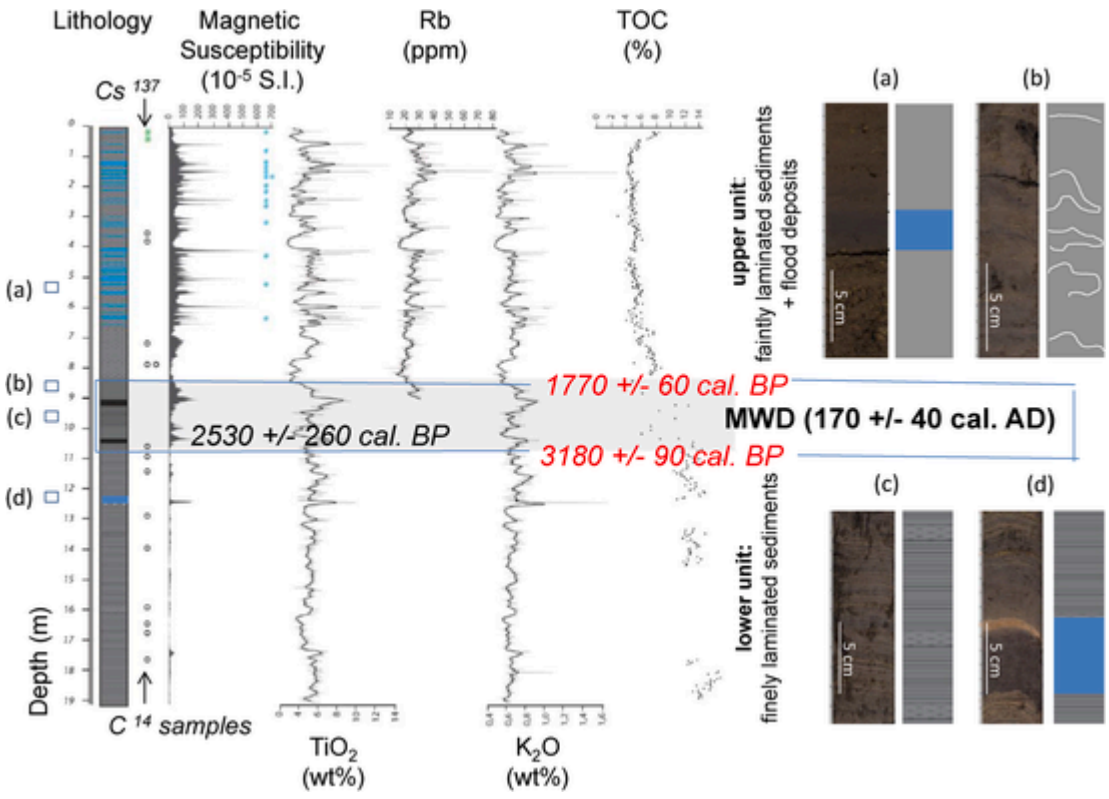

Fig. 9. The lithology and chronology of the sediment core from Lake Aydat in the FMC highlighting the intercalation of an erosive mass wasting deposit (MWD) between the lower and the upper units rich in diatoms and flood layers (blue horizons), respectively. The age-depth model published in Lavrieux et al. (2013a) rely on two ^{137}Cs peaks (green stars), radiocarbon samples (white circles), and historical flood events (blue dots). The digital images of the core lithology (right panel) are showing typical sedimentary facies of the upper unit (a), the MWD (b & c) and the lower unit (d). The MWD is characterized by massive (black layers), folded and laminated deposits bearing both high values and variable contents in terrigenous and organic material. (For interpretation of the references to colour in this figure legend, the reader is referred to the Web version of this article.)

and one in TA-17-01 are in addition identified (Fig. 7). These fine-grained layers are centimetric to pluricentimetric in thickness. The lower unit is also characterized by up to 19 event layers clearly visible on CT-scans in both cores TA-17-01 and −04 (white layers labelled L1 to L19 in Fig. 7). These layers are characterized by higher density than background sediments. Two of these event layers are coarser sandy layers capped by organic debris (L5 and L16) and are easily identified visually between 52 and 54 cm core depth and 107 and 108 cm core depth. These two sandy layers L5 and L16 are matching reflections Ra and Rb on 14 kHz seismic profiles, respectively (Figs. 5c and 7). Three AMS radiocarbon ages at 52 cm, 60 cm and 108 cm core depth in TA-17-04 are in chronological order and allow dating L5 at AD 605 ± 45) and L16 at 2730 ± 30 cal. BP (or 780 ± 30 BC), respectively (Figs. 7 and 8). Radionuclide dating in the upper part of core TA-17-04 (Fig. 7)) suggest a higher sedimentation rate in the upper sedimentary unit (0.36 cm/year) compared with the lower unit (Fig. 8): 0.25 cm/year above 40 cm depth and 0.04 cm/year between 54 cm and 108 cm depth according to calibrated radiocarbon ages. The ^{137}Cs activity was identified from 30.5 cm depth in Lake Tazenat (Fig. 8). Maximal concentration at 11.5 cm depth (320 ± 4 Bq.Kg^{-1}) was attributed to the AD 1986 fallout (Chernobyl accident). Radiocesium peak detected at 19 cm depth (190 ± 2 Bq.kg^{-1}) in association with ^{241}Am fallouts (6 ± 0.8 Bq.kg^{-1}) was attributed to the AD 1963 thermonuclear tests. Log ^{210}Pb$_{ex}$ activities significantly decreased with depth according to a linear regression (r^2 = 0.95). The CIC model applied to date this sequence is in agreement with the ^{137}Cs age depth model. According to the ^{210}Pb model, fallouts associated to Chernobyl were dated in 1986 ± 5 years and thermonuclear test was dated in 1963 ± 2 years and the detection of radiocesium in 1950 ± 25 years. A very low apparent mean sedimentation rate between 40.5 cm depth and L5 (at 54 cm depth) in core TA17-04 is observed. The latter could result from the remobilization of sediments during the emplacement of the coarse grained sand layer L5 (Fig. 7). This L5 layer was thus possibly an erosive turbidite. This turbidite can be correlated with Ra horizon visible on seismic profile basin ward from MWD2 (Fig. 5c). It is also likely that core TA-17-04 was stopped by a sandy turbidite below 108 cm depth similarly associated with MWD4 and developing high-amplitude Rb horizon on 14 kHz seismic data (Fig. 5c).

In core TA-17-01 and below L10 at 80 cm depth, the CT-scan data clearly illustrate (Fig. 7) a package of contorted laminated sediments in between a dense and massive basal layer (102–98 cm core depth), and a massive but less dense upper layer (81–78 cm core depth). Although these particular sedimentary facies were possibly influenced by coring disturbances, they allow calibrating the acoustic facies of MWD3 (Fig. 5a). The age of MWD3 can be estimated by the stratigraphic correlation of L10 on both cores and the calculated age of event L10 in core TA-17-04 (2255 ± 60 cal. BP) when calculating an age–depth model using CLAM software and combining radionuclide with radiocarbon data (Fig. 8).

Between 36 cm (matching L2) and 10 cm core depth in TA-17-01 a syn-sedimentary fault is, in addition, clearly visible on the CT-scan data (Fig. 7). This is suggesting either that lacustrine sediments from both sedimentary units were recently exposed to deformations and/or differential compaction at this location in Lake Tazenat, or that this feature is also related with sediment deformation during coring operations.

4.2. Lake Aydat

In Lake Aydat, the central basin reaching 15 m water depth (Fig. 3c) is today surrounded by steep lateral slopes made of outcropping

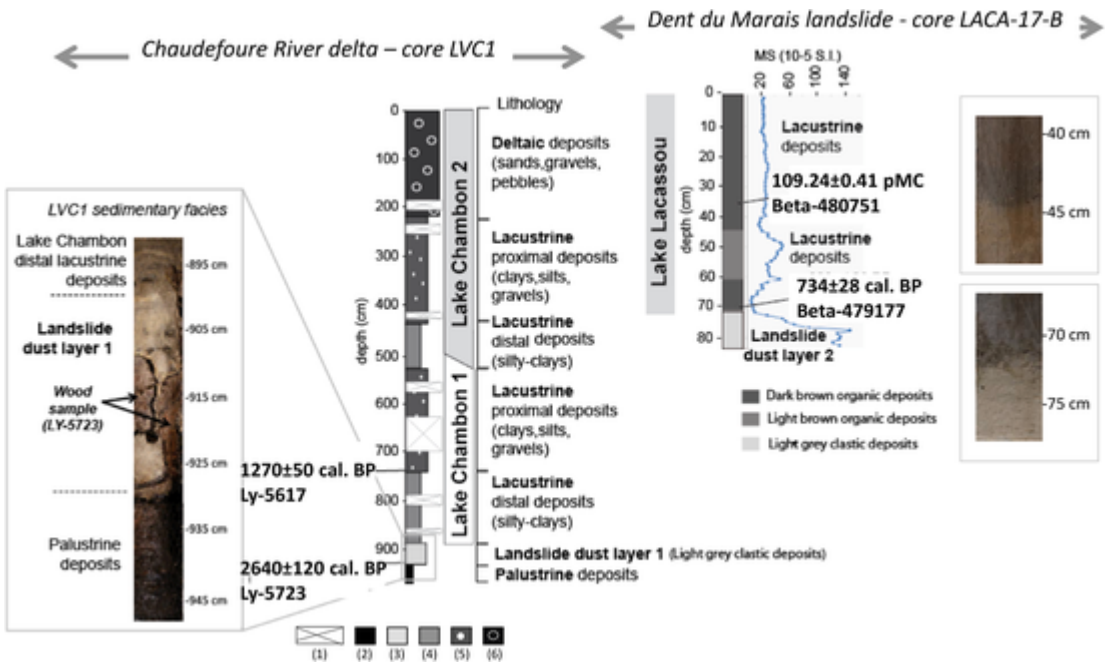

Fig. 10. Lithology of the sediment core from Lake Lacassou (LACA; this study) in the FMC, and correlation with the sediment sequence LVC1 from the Chaudefour River delta (from Gay, 1995) based on available radiocarbon dates, and on the identification on pictures of unusual light grey dust layers in both cores attributed to the impacts of two successive landslides at the Dent du Marais site, as discussed in the text. Changes in the sedimentary facies in core LACA-17-B and selected pictures (right panel) are illustrating a landslide dust layer 2, and lacustrine deposits characterized by variable colours and magnetic susceptibility values. Changes in the sedimentary facies in core LVC1 at the base of the Lake Chambon 1 sediment sequence (left panel) illustrate the landslide dust layer 1 above the palustrine deposits, where a wood sample between 925 and 915 cm core depth was radiocarbon dated. The onset of Lake Lacassou is dated by radiocarbon just above the Landslide dust layer 2 at the Dent du Marais landslide site, and is contemporaneous to the onset of the present day Lake Chambon (Lake Chambon 2 sediment sequence). The LVC1 core lithology (from Gay, 1995) is composed by coring gap (1); palustrine deposits (2); landslide dust layer (3); lacustrine laminated deposits (4); lacustrine deltaic deposits (5) and deltaic deposits (6). (For interpretation of the references to colour in this figure legend, the reader is referred to the Web version of this article.)

Table 1
Results from radiocarbon dating of macrofossil remains from selected intervals in cores retrieved from the sediments of Lake Tazenat, Lake Lacassou (this study) and Lake Chambon (from Gay, 1995) in the FMC. Calibrations were done using IntCAL13. Abbreviation pMC = percent Modern Carbon. Radiocarbon dates were made by AMS for lakes Tazenat and Lacassou.

Lake	Core	LabID	Depth (cm)	Material	δ13C (‰)	Age (BP)	Error	2 sigma range
Tazenat	TA-17-04	Beta-481416	52	Plant fragments	-28.1	1450	30	1300-1390 cal. BP
Tazenat	TA-17-04	Beta-477371	60	Plant fragments	-28.0	1560	30	1386-1530 cal. BP
Tazenat	TA-17-04	Beta-481417	108	Plant fragments	-18.7	2580	30	2700-2762 cal. BP
Lacassou	LACA-17-B	Beta-480751	38	Plant fragments	-26.1	109.24 ±0.41 pMC		-50 cal. BP (AD 2000 ± 2)
Lacassou	LACA-17-B	Beta-479177	72	Plant fragments	-24.7	820	30	686-784 cal. BP (AD 1215 ± 50)
Chambon	LVC1	Ly-5617	740	Bulk sediment	--	1360	55	1180-1365 cal. BP
Chambon	LVC1	Ly-5723	905-925	Wood fragments	--	2585	80	2426-2853 cal. BP

bedrocks, irregular subaquatic slopes produced by the lava flow (NE border of the basin) and more regular slopes produced by the Veyre river delta front (SW border). The interpolated bedrock topography below Lake Aydat (Fig. 3d) is characterized by a marked canyon incised by the Veyre River before the formation of the lake. The lava flow formed a wall up to 15 m high damming the canyon towards the NE. Underneath the Veyre delta forets and topsets, the bedrock is, on the contrary, regularly inclined towards the NE.

The basin fill isopach map of Lake Aydat (Fig. 11, upper panel) derived from the subtraction of the bedrock topography and the lake bathymetry is the thickest (>30 m) in front of the wall formed by the lava flow. Lacustrine sediments are focused within the canyon formed by the former Veyre River and are rapidly getting finer laterally. When including the Veyre delta topsets and forests deposits that progradated into a slightly larger palaeo-lake, a total volume of ca. 3.5 10^6 m^3 of sediments trapped in Lake Aydat is estimated.

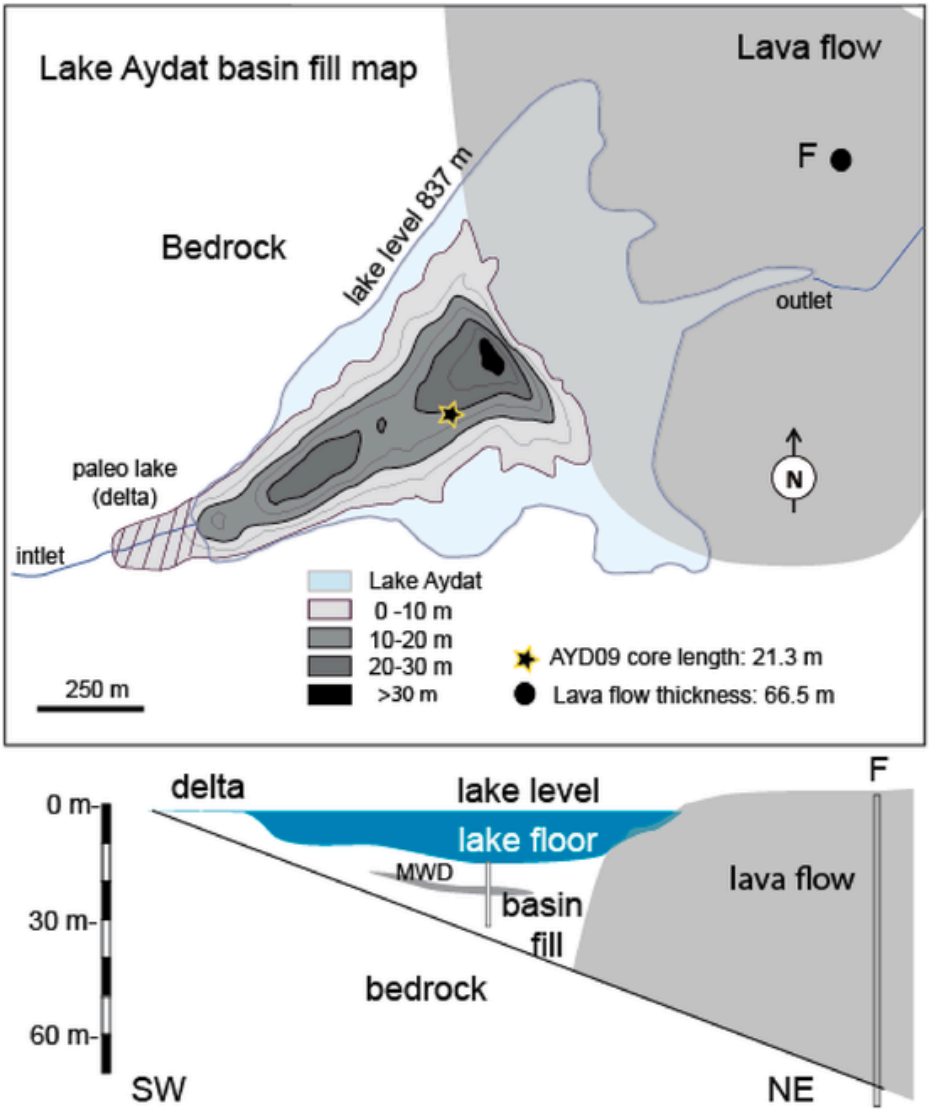

Fig. 11. Map of the basin fill thickness of Lake Aydat in the FMC, including the Veyre delta (upper panel) and a synthetic stratigraphy illustrating the possible extension of its mass wasting deposit (MWD) which originated from the Veyre delta front, and expends in the central basin.

The core AYD09 was retrieved near the axis of the palaeo-canyon at about 250 m from the lava flow wall where sediments are the thickest (Fig. 11, lower panel). This suggests that the bedrock is about 20 m below the lake floor at this location, i.e. only 1 m below the base of core AYD09. Such geomorphological context explains high sedimentation rates calculated by Lavrieux et al. (2013a) for AYD09: 0.2 cm/yr in the lower unit and 0.4–0.6 cm/yr in the upper unit.

In between these two laminated units (1076–829 cm core depth) a MWD is reworking ca. 2.5 m of lacustrine sediments characterized by high and variable MS values, TOC contents (between 2 and 14%) and TiO_2 (between 0.2 and 10 wt%) contents (Fig. 8). As mentioned in Lavrieux et al. (2013a), this MWD contains several disturbed layers (with folded sediments, Fig. 9b) and a 1 m thick well-stratified sequence (Fig. 9c) appearing slightly deformed but exactly repeated. This MWD also developed microfaults at the top of the lower unit. One organic debris sampled near the base of this MWD gave an age of 2530 ± 260 cal. BP, while the AYD09 age depth model indicate that underlying in situ sediments are ca. 3200 years old and that overlying in situ sediments are ca. 1800 years old (Fig. 9). This MWD is thus an erosive event that can be dated to 1780 ± 40 cal. BP (AD 170 ± 40).

Gas-rich sediments in Lake Aydat are preventing any propagation of seismic signal in its basin fill with either a 12 kHz source (Lavrieux et al., 2013a) or a 4 kHz source (Fig. 6a and b). It is thus hard to precisely localize the source area of the MWD sampled in core AYD09. Morphological anomalies were however observed at the lake floor, just in front of the Veyre River delta around 13 m water depth (Fig. 6a). This suggests that the Veyre delta foreset and bottom set beds were once exposed to subaquatic slope failure and then capped by more recent lacustrine deposits.

4.3. Lake Chambon

A geophysical survey of Lake Chambon geomorphology based on ca. 700 m of sub-bottom profiling with a 14 kHz acoustic source (Fig. 4a) failed to image the basin fill geometry because gas-rich sediments absorbed the acoustic signal (Fig. 6c). A small acoustic window was however found on a small ridge delimitating the southern and northern sub-basins of Lake Chambon and revealed one low-amplitude reflection (labelled R1) ca. 50 cm b.l.f. draping the lake floor morphology (Fig. 6c).

On these sub-bottom profiles, Lake Chambon bathymetry reached a maximum depth of 4.25 m in the northern sub-basin, suggesting either a higher lake-level compared to the 2009 mapping campaign (Fig. 4b) and/or dredging operations to preserve this touristic site from a complete siltation. Variable maximal bathymetry documented at the end of

Fig. 12. Illustration of lacustrine landscape changes in our study are in the FMC as discussed in the text. (a) Old post card from Lake Chambon in 1927 showing the high lake-level flooding of Lake Lacassou. (b) Google-Earth 3D view of Lake Chambon in 2015 and location of the 1927 high lake-level (yellow dotted line). (c) Picture taken during the 41st International Moor Excursion in the FMC in 2017 with the Lake Pavin palaeo-outlet situated above the present maar lake-level. (For interpretation of the references to colour in this figure legend, the reader is referred to the Web version of this article.)

the 19th century (5.8 m; Delebecque, 1898), in March 2009 (3 m, cf. Fig. 4b) and in June 2017 (4.25 m, cf. Fig. 6c), together with old photographs from Lake Chambon highlighting much higher shorelines than today (Fig. 12a) suggest that this lake is fluctuating seasonally and that its sedimentation and water level are largely controlled by the Chaudefour River.

4.4. Lake Lacassou sedimentation

Lake Lacassou is the largest lake identified above the Dent du Marais landslide deposits and is characterised by a 2-m deep, 40-m wide, circular basin (Fig. 4c). Both gravity cores LACA-17-A (76 cm long) and LACA-17-B (82.5 cm long, Fig. 11) revealed a fine-grained light grey massive clastic layer capped (above 70.5 cm core depth) by fine grained and brownish sediments containing few organic macro-remains. The clastic base of core LACA-17-B is characterized by high MS values (up to 140 10^{-5} S.I.). Above this clastic base, a lower unit (from 70.5 to 60.5 cm core depth) made of dark-brown and homogenous organic rich lacustrine deposits is showing minimum MS values (<10 10^{-5} S.I.). The middle unit (from 60.5 to 44 cm core depth) made of light-brown and homogenous lacustrine deposits, is characterized by slightly higher MS values (up to 60 10^{-5} S.I.). The upper unit (from 44 to 0 cm core depth) is made of dark brown and homogenous organic-rich lacustrine deposits showing low MS values (around 20 10^{-5} S.I.). As shown in Fig. 11 and Table 1, two organic macro-remains sampled at 70.5 cm and 37 cm core depth in LACA-17-B were dated to AD 1215 ± 50 and of post 0 BP (109.24 ± 0.41 percent Modern Carbon, pMC), respectively. Once reported as percentage of the modern reference standard (BetaCal 3.21 HPD method from INTCAL 13, NHZ1), this modern sample at 37 cm in core LACA-17-B was likely a living material around −50 cal. BP (ca. AD 2000). Thus, this sample was probably remobilized from the lake subsurface during coring operations.

5. Discussion

5.1. Lake Tazenat sedimentation mode and chronology of slope failure events

The palynological contents and sedimentological data from core TA-96 (Juvigné and Stach-Czerniak, 1998) revealed that a fine-grained and organic rich lacustrine sedimentation prevailed in Lake Tazenat central basin since the early Late-Glacial period. Available bathymetric and sub-bottom profiling data offshore the Rochegude River delta are not showing any typical subaquatic delta geometries, but show only steep slopes and a morphological step below 39 m water depth where an active and erosive channel is developed down to 59 m water depth. Sedimentation in this maar lake was thus characterized by limited sediment supply from its tributary since the crater formation, but tributary floods may have favoured the development of hyperpycnal flows (Mulder and Chapron, 2011) down to the central basin of Lake Tazenat. Hyperpycnal flows generated by flood events can produce lateral variations in depositional rates in the central basin of Lake Tazenat and explain the divergent fill observed on N–S seismic profiles. In this context, L1 to L4 and L6 to L18 event layers identified on CT-scan data from cores TA-17-01 and TA-17-04 in the lower unit can be interpreted as distal hyperpycnal flood deposits (Mulder and Chapron, 2011). The sediment source

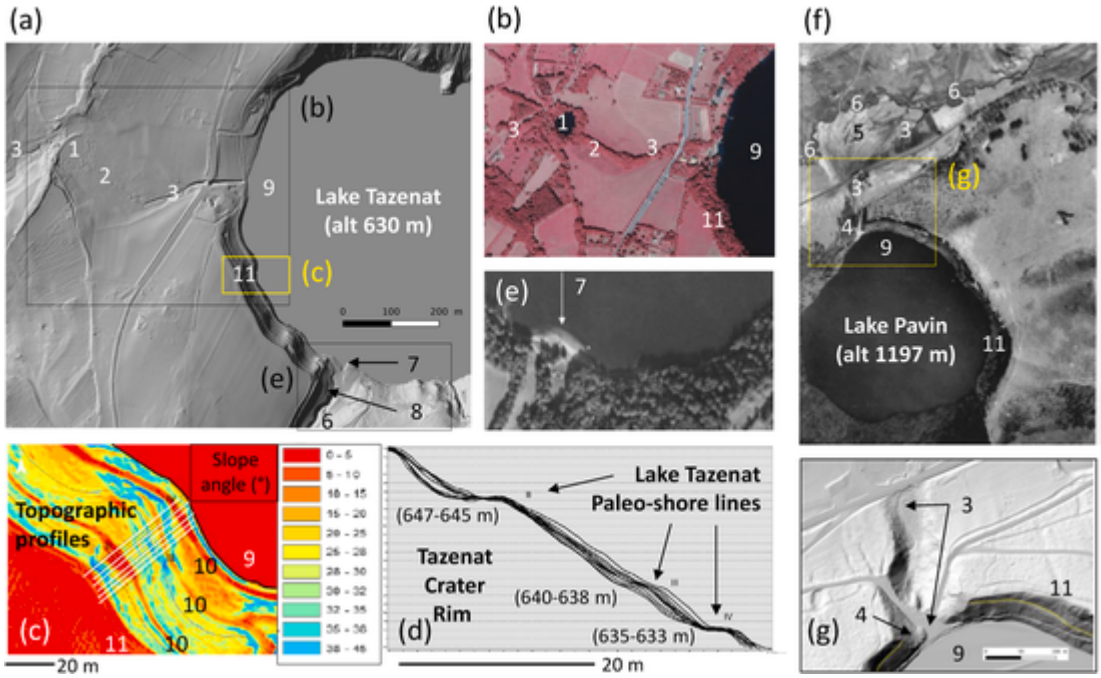

Fig. 13. Detailed geomorphologies of the maar Lake Tazenat and Lake Pavin in the FMC suggesting changes in lake-levels. (a) LIDAR image of Lake Tazenat crater rim. (b) Aerial photograph of Lake Tazenat in 1985. (c) Slope map of LIDAR data illustrating the signature of palaeo-shorelines and the location of topographic profiles illustrated in (d) to document palaeo-shoreline altitudes. (e) Aerial photography of Lake Tazenat tributary delta in 1946. (f) Aerial photography of Lake Pavin in 1955. (g) LIDAR image of Lake Pavin crater rim near the lake outlet. In all these pictures the images numbers are indicating main morphological features: 1 pond, 2 peat bog, 3 outlet, 4 palaeo-outlet, 5 outwash fan, 6 stream, 7 delta, 8 palaeo-delta, 9 maar lake, 10 palaeo-shoreline, 11 crater rim.

of these silty flood deposits may come from the 12 m incision of the Rochegude River documented by Juvigné and Stach-Czerniak (1998). The absence of similar deposits in the upper unit may result from the construction of the Rochegude pond acting as a sediment trap (De Crespin de Billy et al., 2000), and/or land-use changes inducing a new sedimentation pattern around AD 1945 (Fig. 8). New agriculture practices after the World War II may have favoured a sedimentation dominated by authigenic sediment supply, favouring trophic-level changes (including cyanobacteria blooms, Foucher et al., 2020; Legrand et al., 2019). Subaqueous morphological steps are frequent features in maar lakes (Chapron et al., 2010) and generally resulting from syn-eruptive collapse masses (Thouret et al., 2016). In Lake Tazenat, since the morphological step is located offshore the tributary (Fig. 2c) and just downstream steep rocky slopes visible on LIDAR data (Fig. 13a and e), it may have favoured the accumulation of some deltaic and slope deposits as suggested by Juvigné and Stach-Czerniak (1998). The authors also documented a palaeo-delta locally preserved from erosion and exposed above the tributary channel. This palaeo-delta is located at 635 m altitude at ca. 50 m upstream from the present-day delta in Lake Tazenat (Fig. 13a) and can be correlated with a palaeo-shoreline observed between 633 and 635 m altitude (Arricau, 2020). This suggest that the third palaeo-shoreline identified within the crater ring of Lake Tazenat (3–5 m above the present-day lake-level) occurred either during a long period of time or during a period when the Rochegude stream was characterized by significant sediment load. Further studies are required to date this former lake-level.

Sub-bottom profiling revealed that small sized MWDs are also frequently observed stacked at the edges of the basin and originating essentially from the western, north-western, eastern and south-eastern slopes of Lake Tazenat (Fig. 5). Following Mulder and Cochonat (1996), high-amplitude reflections Ra, Rb and Rc identified on 14 kHz profiles down slope from MWD2, MWD4 and MWD5, respectively, are interpreted as distal turbidites laterally associated with MWDs. Ra was sampled in cores TA-17-04 and consists in a 2 cm thick sandy layer with a unimodal distribution (d50 between 280 and 290 μm, Fig. 7). This sandy layer is very similar to S1 unimodal sandy layer documented by Juvigné and Stach-Czerniak (1998) in core TA-96 (Fig. 8).The three other sandy layers documented in core TA-96 (S2 to S4 in Fig. 8) were also characterized by an unimodal distribution (d50 between 250 and 500 μm) and might thus also correspond to distal turbidites associated with former MWDs.

At least five generations of slope failure events are documented during the Late Holocene in Lake Tazenat. The most recent event (MWD1) is not dated yet and should be sampled by gravity cores to confirm if several slopes were reworked simultaneously or not. MWD2 is characterized by multiple slopes failures (Fig. 5) and dated to AD 600 ± 25 by the radiocarbon date above the sandy turbidite layer L5 in core TA-17-04 (Table 1, Fig. 7). This event is contemporaneous to a seismite layer identified by Vernet (2013) in archaeological excavations both in paludal deposits from the Limagne basin North of Clermont-Ferrand city and above the Sarlièvе palaeo-lake sequence from the Limagne basin (south of Clermont-Ferrand). Based on stratigraphic and archaeological data, this regional seismite occurred just above a major historical flood layer in AD 580 (Vernet, 2013). It is thus likely that multiple subaquatic slope failures associated with MWD2 and L5 turbidite in Lake Tazenat were triggered by a regional earthquake soon after AD 580. Similarly, MWD3, dated 2255 ± 60 cal. BP, is characterised by coeval slope failures in Lake Tazenat, suggesting a seismic triggering. Following the same argumentation, coeval slope failures associated with MWD4 and a distal turbidite (horizon Rb and layer L16) suggest a seismic triggering around 2730 ± 30 cal. BP (or 780 ± 30 BC). Long coring is necessary to sample and date either one of the coeval MWD5 or the associated turbidite (horizon Rc). It seems also possible that sandy layers documented by Juvigné and Stach-Czerniak (1998) during the Late Holocene in TA-96 (Fig. 8) are turbidites associated with slope failures. Available radiocarbon dates from TA-96 were obtained from bulk lacustrine sediments (Juvigné, personal communication) and should be considered with caution because of potential radiocarbon reservoir effect in maar lakes (Albéric et al., 2013).

5.2. Lake Aydat delta failure event

Sediment load from the Veyre River coming from the erosion of andosols in the Lake Aydat drainage basin, favoured the progradation of the Veyre delta (Fig. 11) since the lake formation ca. 8500 years ago. Variable trophic levels of Lake Aydat also induced high autochthonous sediment supply since the Early Holocene (Lavrieux et al., 2013a; Legrand et al., 2019). Given its geomorphological setting, lake-level drops were limited by the altitude of the lava flow at the lake outlet. Wet periods documented from periods of enhanced clastic sediment supply in Lake Aydat (Lavrieux et al., 2013a) may have favoured only short phases of higher lake-level and enhanced current at the lake outlet. The Veyre delta subaquatic slopes are, in addition, the only slopes in Lake Aydat exposed to sediment gravity reworking.

In such a context, it is very likely that the erosive MWD sampled in core AYD09 and dated to AD 170 ± 40 resulted from the collapse of the Veyre prodelta. This interpretation is supported by higher content of both clastic sediments (reflected by MS and K_2O values) and very variable values of TOC in lacustrine sediments from the MWD (Fig. 9). However, it is not possible to tell if this MWD resulted from changes in sedimentation mode during the Roman period, since this period is poorly documented in the FMC and not sampled in sediment cores from Lake Aydat. This MWD may have been related to a delta slope overloading and failure consecutive to a period characterized by strong sediment inputs from the catchment. The climatic and/or human driver behind these inputs remains unclear in the absence of dated sediment during this period. The absence of any other MWDs or turbidites associated with MWDs in core AYD09, and in particular the absence of any specific deposits in relation with the AD 580 regional earthquake, suggest that all unstable slopes along the Veyre delta were purged in AD 170 and have remained stable since then.

5.3. Formation and evolution of Lake Chambon and Lake Lacassou

Since Lake Lacassou was created in a topographic depression formed by the Dent du Marais landslide, organic-rich lacustrine sedimentation in LACA-17-B began soon after the emplacement of the debris avalanche deposits. The onset of organic lacustrine sediments above 70.5 cm core depth in LACA-17-B dated to AD 1215 ± 50 can therefore provide a minimum age of the Dent du Marais landslide. The fine-grained and massive light grey clastic base of core LACA-17-B is interpreted as derived from the dust-cloud particles produced by the Dent du Marais landslide. The onset of organic-rich lacustrine sedimentation above this dust deposit would thus mark the onset of the newly formed lake system on top of the Dent du Marais landslide deposit. Similar dust deposits capped by lacustrine sediments were documented in cores from several Swiss lakes formed or impacted by large rock avalanches (Deplazes et al., 2007; Knapp et al., 2017). According to Vidal et al. (1996), the Dent du Marais debris avalanche was characterized by a high mobility as evaluated by its coefficient of friction (H/L = 0.114, where H is the altitude difference between the crest of the slide scar and the altitude of the front of the avalanche and where L is the maximal distance of material transported by the avalanche). According to Pollet and Schneider (2004), dynamic disintegration processes during rock avalanching can led to the complete disintegration of the rock mass, due to shearing and dilatancy processes reducing particle size during a rapid transport. According to Pollet et al. (2005), the absence of confinement at the boundaries of the rock mass allows also the debris to spread in the valley and further favor particle size reduction. High-speed movements of large rock masses are in addition often characterised by dust dispersions. Debris avalanche deposits are therefore typically consisting in mega-blocks developing hummocky topographies and these blocs are imbedded within a fine grained matrix (Vidal et al., 1996). The matrix proportion increases downslope during debris avalanche progression and becomes dominant in the distal deposits. Matrix facies are generally composed of block material and eroded materials at the base of the avalanche during transportation. In the Dent du Marais avalanche debris deposits, the greyish fine grained matrix facies is composed of incoherent pyroclastites partly resulting from the progressive fragmentation of blocks during transport (Vidal et al., 1996). The dust layer sampled at the base of core LACA-17-B and illustrated in Fig. 10 is thus interpreted as resulting from dust dispersions in the distal deposits of the Dent du Marais debris avalanche developing hummocks around Lake Lacassou and at the floor of Lake Chambon (Fig. 4b).

Less than 1 km from Lake Lacassou, core LCV1 retrieved in the Chaudefour River delta next to Lake Chambon (Fig. 4) is also characterized by a striking light grey massif and fine grained layer (Fig. 10). This layer sampled between 9.3 and 9 m core depths above palustrine deposits is covered by Lake Chambon lacustrine deltaic deposits. According to Gay (1995) Lake Chambon deposits (LCV1) are consisting, from the bottom to the top in: laminated silty clays (lacustrine distal deltaic facies, 9–7.4 m depth), evolving into clays, silts and gravels (lacustrine proximal deltaic facies, 7.4–5.25 m depth), and then another lacustrine distal deltaic facies (5.25–4.4 m depth) covered by a lacustrine proximal deltaic facies (4.4–2.1 m depth) that is capped by sands, gravels and pebbles from the Chaudefour River delta (topset beds facies, 2.1 m depth to surface). Two radiocarbon samples from LCV1 drilling site (Fig. 10) were used by Gay (1995) and Macaire et al. (1992, 1997) to constrain the age of Lake Chambon formation following the development of the Dent du Marais landslide: a wood sample in 9.25–9.05 depth in the LCV1 drill core dated to 2640 ± 210 cal. BP, and a sample of peat deposits at 7.4 m core depth dates to 1270 ± 100 cal. BP (AD 680 ± 50). Palynological analyses with low-resolution sampling interval from core LVC1 from the Lake Chambon deltaic sequence are typical from the Subatlantic period and characterized by cereals. This is suggesting human impact and land use in the study area (Gay, 1995). Available chronological data from the LVC1 drill site are thus suggesting that the landslide dust layer sampled above the palustrine deposits and below the lacustrine deposits occurred during the Late Holocene (i.e. much earlier than revealed by the Lake Lacassou sequence).

The time gap between the radiocarbon age obtained from the Lacassou sequence (735 ± 50 cal. BP) at 2 sigma (AD 1215 ± 50), or 720 ± 25 cal. BP (AD 1230 ± 25) at 1 sigma (with a likelihood of 98%) and the one from the wood debris sampled at the base of core LVC1 in Lake Chambon (2640 ± 210 cal. BP at 2 sigma), suggests the Dent du Marais landslide deposits may have resulted from two successive slope failure events in the Chaudefour valley. The first event, characterized by a dust layer dated to 2640 ± 210 cal. BP in the core of LVC1, can be linked to a landslide having dammed the valley, creating Lake Chambon 1 (Fig. 10) by flooding an ancient marsh inferred by paludal deposits. A second landslide occurred almost 2000 years later favoured the nucleation of Lake Lacassou in AD 1215 ± 50. Following this second landslide, Lake Chambon 1 may have been changed into the present-day Lake Chambon (i.e. Lake Chambon 2 in Figs. 10, 14 and 15). The geomorphology of Lake Chambon may thus result from the progressive development of the Chaudefour delta in a lacustrine basin dammed by two successive landslides originating from the Dent du Marais area during the Late Holocene. Rockfalls and landslides in glacial or volcanic valleys are generally favoured by active tectonic setting and environmental changes following deglaciations (Macaire et al., 1992; Vidal et al., 1996; Schneider et al., 2004; Deplazes et al., 2007; Nepop and Agatova (2016); Defive et al., 2019) and can result either from earthquakes, volcanism, fluvial incision, heavy rainfalls and freeze-thaw cycles, or a combination of these factors. The Dent du Marais landslide is the largest of the MCF and is located above the Jassat fault (Vidal et al., 1996) at the edge of the Late-Glacial Tartaret stratovolcano (Fig. 4a). This Late Holocene rock avalanche deposit was thus favoured by its geological context.

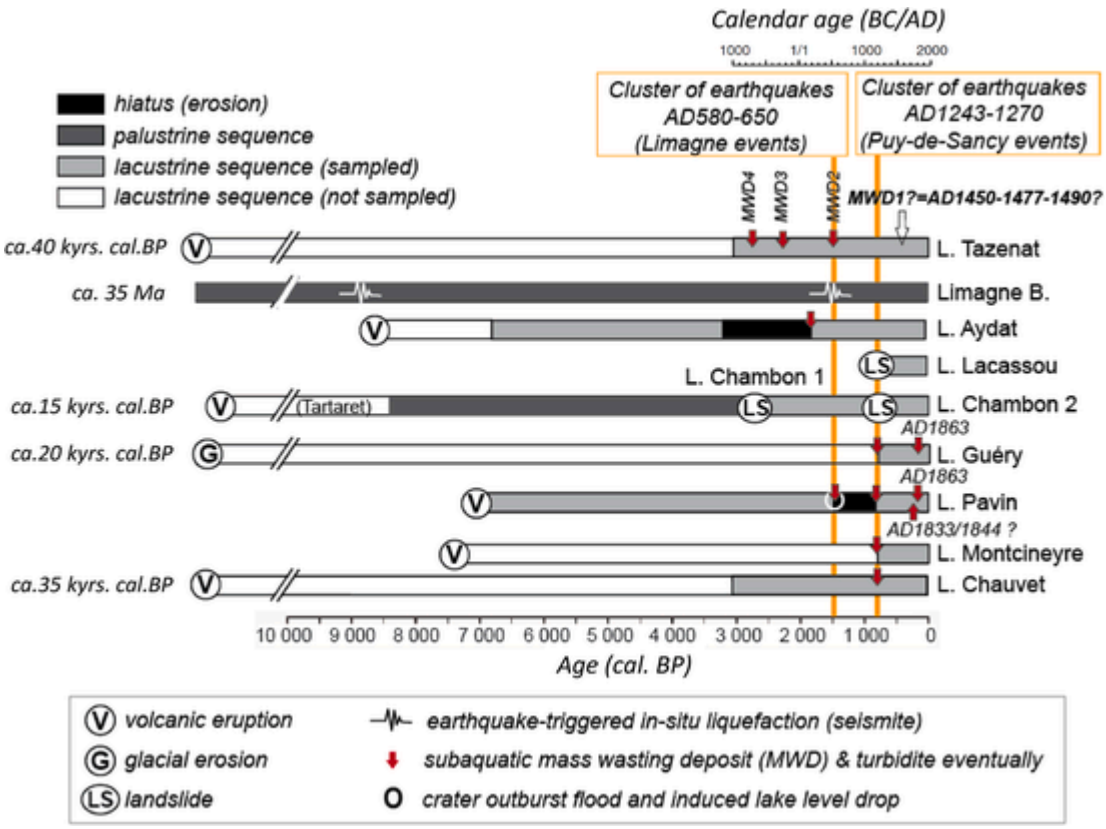

Fig. 14. Synthetic diagram illustrating the origin and age of Holocene lacustrine and palustrine sequences documented in the French Massif Central, together with a schematic regional event stratigraphy highlighting the chronology and stratigraphic record of historical earthquakes and clusters of palaeo-earthquakes as detailed in the text. Seismites (ball and pillow structures) from the Limagne Basin were documented by Vernet (2013). Some landslide deposits were erosive and produced a chronological hiatus (black colour) in lacustrine sequences. (For interpretation of the references to colour in this figure legend, the reader is referred to the Web version of this article.)

5.4. Regional event stratigraphy and palaeo-seismicity

Subaquatic landslides in glacial, tectonic or volcanic lakes can be triggered by peak ground acceleration (PGA) during an earthquake, especially along steep slopes and near deltas where gas-rich sediments are generally unstable (Strasser et al., 2013; Van Daele et al., 2015; Chapron et al., 2016b). Lake-level changes in maar lakes are also frequent, either progressive or abrupt, and can induce changes in sediment pore pressure leading to slope failures (Moernaut et al., 2010; Chassiot et al., 2016a) and eventually develop catastrophic crater outburst floods or limnic eruptions in meromictic maar lakes (Chapron et al., 2010; Chassiot et al., 2016a). In the crater rim of Lake Tazenat, exposed palaeo-shorelines and an exposed palaeo-delta (illustrated in Fig. 13c and d, and mentioned by Juvigné and Stach-Czerniak, 1998) are suggesting that the lake-level of Lake Tazenat successively dropped from ca. 16 m; 9 m and 4 m (Fig. 13d). It is thus likely that the five generations of MWDs observed on seismic profiles in Lake Tazenat (Fig. 5) were favoured by changes in sediment stability following the four generations of lake-level drops documented by palaeo-shorelines, the palaeo-delta and the present-day shoreline. Dating these morphologies of the crater rim are needed to eventually correlate them with documented MWDs and turbidites in cores TA-17-04; T1-17-01 and TA-96 (Fig. 8). In maar Lake Pavin, Chassiot et al. (2016a, c) reconstructed an abrupt lake-level drop (9 m above the present lake-level) following the AD 590–650 MWD (Fig. 15) that was associated with violent and erosive waves (Chapron et al., 2012), and a crater outburst flood that formed an outwash fan at the confluence from the lake outlet with the Pavin River. Miallier (2020) suggested that Lake Pavin remained at its present elevation (1197 m a.s.l.) since the beginning of the 18th century but documented a palaeo-outlet ca. 4.8 m above the present lake-level (Figs. 12c and 13g). It is thus likely that the AD 1290–1350 MWD documented in Lake Pavin in association with violent waves by Chapron et al. (2012) and Chassiot et al. (2016a, c) was also associated with a crater outburst flood and a ca. 4.8 m abrupt drop of the lake-level that bypassed the former outlet developed between AD 590–650 and AD 1290–1350 (Figs. 12c, 13g and 15). In both maar Lakes Tazenat and Pavin, it is thus likely that lake-level changes have changed lacustrine sediment stability and favoured subaquatic slopes failure events triggered by earthquakes.

The best arguments to associate subaerial or subaquatic landslides with an earthquake is to identify active faults, and to date the landslides and demonstrate that several slopes failures events occurred simultaneously, or within a short time period (cluster of earthquakes) at a regional scale in a single lake (in several sub-basins) or in several lacustrine or marine basins (Chapron et al., 2006, 2016b; Strasser et al., 2013; Van Daele et al., 2015) since these are the typical signatures of historical earthquakes in the environment. Lake basins are however neither simple nor stable natural seismographs essentially because:

(i) Slope overloading in lakes following changes in sedimentation modes or rates (in relation with environmental changes due to climate or human impact, cf. Girardclos et al., 2007; Chapron et al., 2016a; Chassiot et al., 2016b) can trigger slope failure events, and the history of former slope failure events can impact the sensitivity of a lake to following earthquakes during a relatively long period of time (i.e. when unstable slopes are purged and if sedimentation rates are low for example);
(ii) Complex propagation of seismic waves in mountainous region are difficult to model due to topographic effects and site effects that are strongly impacting PGA (and thus triggering landslide), and

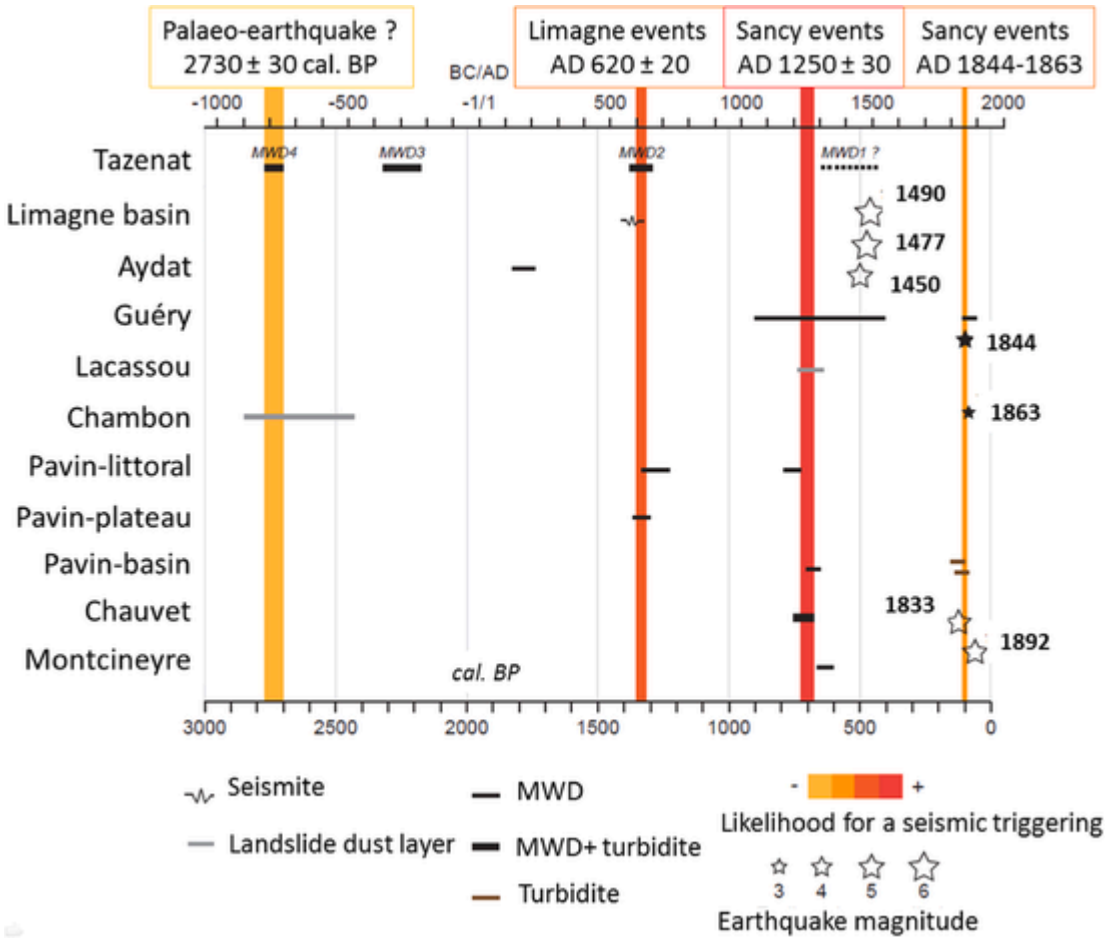

Fig. 15. Synthetic plot illustrating the dating uncertainties of sedimentary event layers in selected lakes of the FMC, and the regional event stratigraphy of historical earthquakes and clusters of palaeo-earthquakes as detailed in the text. Seismites (ball and pillow structures) from the Limagne Basin are documented by Vernet (2013). A sedimentary event is made of a landslide dust layer (grey bars), of Mass Wasting Deposits (MWD, black bars), of MWDs and turbidites (black bold bars), or turbidites (brown bars). Historical earthquake dates (number in AD) and magnitudes are indicated by the size of white stars and numbers. The likelihood for a seismic triggering is linked to the number and coeval regional sedimentary events from the studied lakes and from the Limagne basin. (For interpretation of the references to colour in this figure legend, the reader is referred to the Web version of this article.)

consequently it is complicated to estimate the precise location and strength (or magnitude) of palaeo-earthquakes based only on the size or numbers of contemporaneous MWDS in lakes at a regional scale (Chapron et al., 2016).

Former limnogeological studies conducted on lakes located south of the Puy-de-Sancy stratovolcano (Fig. 1) have documented a several sedimentary events related to slope failures, earthquakes and/or crater outburst floods over the last two millennia (Chapron et al., 2010, 2012, 2016a; Chassiot et al., 2016a, b,c). The following synthesis of radiocarbon-dated sedimentary sequences from the Lakes Pavin, Chauvet, Guéry, Montcineyre allows some regional correlations with the Lakes Tazenat, Chambon and Lacassou sedimentary records and provide new evidences for palaeo-hazards in the FMC.

As shown in Fig. 14, the sedimentary sequences from the plateau and the central basin of Lake Pavin and covering the last 7 kyrs, are notably characterized by two erosive MWDs dated to AD 620 ± 30 (Chassiot et al., 2016a) and AD 1280 ± 20 (Chassiot et al., 2016b), one of them having triggered a crater outburst flood following an abrupt lake-level fall (Chassiot et al., 2016b). In addition, several turbidites recorded in the upper sequence were related to historical earthquakes occurring during the late 19th century (Chassiot et al., 2016a, b). The available sedimentary sequence of maar Lake Chauvet is covering the last three kyrs and revealed a major MWD (AD 1240 ± 40) evolving into a thick turbidite in the central basin (Chapron et al., 2012, 2016a, Chassiot et al., 2016b). The sedimentary sequence from Lake Montcineyre is covering the last 700 years and allows estimating the age of a small lens-shaped MWD (AD 1320 ± 30) identified on seismic profiles (Chapron et al., 2012; Chassiot et al., 2016b). The sedimentary sequence from Lake Guéry documents the last 650 years and contains one recent thin MWD resulting from the construction of a hydroelectric dam in AD 1895 and two older and thicker MWDs dated AD 1860 ± 40 and 1300 ± 250, respectively (Chassiot et al., 2016b). The synchronicity of MWDs in the late 13th century suggests a common trigger and thus allowed the authors to highlight a then-unknown palaeo-earthquake around AD 1300 (Chassiot et al., 2016b).

The most recent historical earthquake from the FMC recorded in lakes is the AD 1863 Mont Dore earthquake (Fig. 15). This event located in the Puy-de-Sancy stratovolcano area (referred hereafter as Sancy event) had an estimated Richter scale magnitude (Mw) of 3.38 ± 0.62 and triggered a MWD (dated to AD 1866 ± 40) in Lake Guéry and a thin silty turbidite (dated to AD 1860 ± 20) in Lake Pavin (Chassiot et al., 2016a, b). A similar thin turbidite in Lake Pavin dated to AD 1825 ± 20 could match either the AD 1844 Chambon-sur-Lac earthquake (a Sancy event) or the AD 1833 Issoire earthquake (Chassiot et al., 2016a). The latter quake was located near the Southern Limagne fault and can be referred as a Limagne event.

The most intense historical earthquakes of the FMC were Limagne events located in the Northern part of the Limagne fault and occurred in clusters in AD 1450, AD 1477 and AD 1490. These events had an esti-

mated Magnitude (Mw) of 6.1 ± 0.3 and a Medvedew-Sponheuer-Karnik (MSK) scale Intensity between IV and VIII, but not recorded within lakes located around the Sancy area (Chassiot et al., 2016b). One of these earthquakes may have, however, triggered the most recent coeval slope failures in the nearby maar Lake Tazenat (MWD1). To address this question, core sampling of MWD1 at several locations in the lake basin and both radionuclide and radiocarbon dating are required to precisely date this event at the transition from the clastic-dominated unit to the organic-rich upper unit (Fig. 8).

In the present study, the landslide evidenced with a dust layer at the bottom of the Lake Lacassou sequence is dated to AD 1215 ± 50, and matches the ages of the MWDs recorded in the surrounding Lakes Pavin, Chauvet, Montcineyre and Guéry (Chassiot et al., 2016; Chapron et al., 2012), which support both a seismic origin for this landslide, and thus the hypothesis of a two-stage slide for the Dent du Marais deposits. This interpretation is in agreement with Vidal et al. (1996) suspecting a tectonic origin of the Dent du Marais landslide in relation with the Jassat strike slip fault. According to these authors, earthquake triggering would not require a strong intensity in Lake Chambon area since the geological formations involved in the Dent du Marais landslide are faulted and developed a cliff of (unstable) volcanoclastic material lying on a clayey substrate. This interpretation is further supported by archaeological investigations on the neighbouring Murol castle highly exposed to earthquake-generated topographic effect (Fig. 4d) revealing unusual failures and collapse structures estimated to the late 13th century (Allios, 2015).

Correlating a new event (i.e., Lacassou dust layer) to this regional historical earthquake also increases its seismic likelihood by slightly rejuvenating its age around AD 1250 ± 20 (Fig. 15). Accordingly, it is likely that a cluster of earthquakes (Sancy events) occurring between AD 1220 and 1280 have triggered the most recent part of the Dent du Marais landslide and subaquatic slope failures in Lakes Montcineyre, Pavin, Chauvet and Guéry. The identification of a palaeo-outlet at Lake Pavin (Figs. 12c and 13g) is also suggesting that this cluster of earthquakes induced an outburst flood and a lake-level drop down to the present-day altitude of this maar lake. New coring and radiocarbon dating in the (less accessible) other small lake nucleated above the Dent du Marais landslide deposit located near Lake Lacassou (Lake Ronces; Fig. 4c) would be necessary to confirm this interpretation and the very recent age (13th centuries) of the second Dent du Marais landslide. The transition from Lake Chambon 1 to Lake Chambon 2 in drilling site LVC1 may also correspond to the intercalation of a fine-grained sequence of lacustrine (silty-clayey) deposits accumulated in a distal deltaic environment (5.25–4.4 m in LVC1) in between two sequences of coarse-grained lacustrine deposits accumulated in a proximal deltaic environment (Fig. 10). No slope failure events are documented around this period within Lakes Tazenat and Aydat, likely because the stability of the slopes was more important following the landslides that took place 700 years ago in Tazenat, and 1100 years ago in Aydat.

A cluster of palaeo-earthquakes is also evidenced in the FMC at the transition between the 6th and 7th centuries (Fig. 15). This cluster includes the seismite documented by Vernet (2013) and is dated to ca. AD 580 in the Limagne area. This earthquake (a Limagne event) is also interpreted as the most probable trigger for coeval subaquatic slope failures in maar Lake Tazenat (MWD2) evolving in the central basin into a sandy turbidite producing reflection Ra on seismic profiles and related to event L5 dated to AD 605 ± 45. In maar Lake Pavin the large slump deposit identified on the subaquatic plateau is dated to AD 620 ± 30 and associated to a sandy layer in a littoral site dated to AD 665 ± 50, and is interpreted as the signature of unusual and violent waves (Chapron et al., 2012; Chassiot et al., 2016a). This slump event was also contemporaneous to a catastrophic outburst flood event in the Pavin river valley resulting from the collapse of a part of the Pavin crater rim that induced a lake-level drop (Chassiot et al., 2016a, b, c). These major environmental changes in Lake Pavin are not associated with any specific events in the nearby Lakes Chauvet and Moncineyre records and are thus interpreted as resulting from a cluster of earthquakes (Limagne events) occurring between AD 580 and 650. The record of a Limagne event in Lake Pavin implies that this lake is highly sensitive to earthquakes, comparing to other lakes in the Puy-de-Sancy area, which is likely due to its steep morphology combined to a landslide-prone crater rim made of juvenile unstable pyroclasts (Chapron et al., 2010; Juvigné and Miallier, 2016; Thouret et al., 2016).

Late Holocene palaeo-earthquakes near maar Lake Tazenat (Limagne events?) are in addition suggested around 2255 ± 60 cal. BP by coeval subaquatic slope failures (MWD3) and associated turbidite (L10 event) and around 2730 ± 30 cal. BP by coeval subaquatic slope failures (MWD4). The likelihood for a seismic origin for MWD4 is enhanced since its age matches the dust layer identified in LVC1 (Lake Chambon), dated to 2640 ± 210 cal. BP (Fig. 15). Additional dating is however needed to confirm this hypothesis and better constrain the timing of this event recorded in both the Sancy and the Limagne regions. Holocene earthquakes are may also have occurred, as suggested by sandy turbidites (S2, S3 and S4 in Fig. 8) documented (but poorly dated) in the central basin of maar Lake Tazenat (Juvigné and Stach-Czerniak, 1998). Long piston coring and radiocarbon dating on organic macro-remains are needed in Lakes Tazenat and Chambon to confirm and date such possible former Limagne events. Early Holocene palaeo-earthquakes (Limagne events?) are also documented by seismites affecting tephra layers in the Limagne paludal sequence between 8850 and 9500 cal. BP (Vernet, 2013) and co-seismic fault movements around 9500 cal. BP in volcanoclastic deposits near the Pariou volcano in the Chaîne -des-Puy (Miallier et al., 2008). As a working hypothesis, we suggest that the lava flow that formed Lake Aydat around 8550 ± 400 cal. BP (Boivin et al., 2009) and the emplacement of the Plate rock fall that formed the Monneaux palaeo-lake around ca. 9500 cal. BP in the Chaudefour valley up stream Lake Chambon may have been associated with (and eventually favoured by) regional earthquakes.

The triggering factor of the large and erosive MWD originating from the Veyre delta dated to AD 170 ± 40 in the central basin of Lake Aydat remains however poorly understood. Environmental changes, human activities and climate variability between ca. 3200 cal. BP and AD 170 are poorly documented in the study area since this time windows was reworked in Lake Aydat (Figs. 9 and 11). In the Lake Pavin central basin two peaks of terrigenous input are, however, identified around 2800-2600 cal. BP and 1800-1600 cal. BP (Chassiot et al., 2018). Since similar fluctuations in Lake Pavin sedimentation around 4100 and 3800 cal. BP and during the Little Ice Age were coeval with the occurrence of floods in Lake Aydat, it is likely that enhanced flooding activity occurred in Lake Aydat before the emplacement of the erosive MWD in 1780 ± 40 cal. BP (i.e. AD 170 ± 40). These periods of enhanced terrigenous supply in Lake Pavin are also matching enhanced flooding activity in the western French Alps (Arnaud et al., 2012) and a higher lake-level phase in western Europe (Magny et al., 2013). It is thus possible that climate changes and enhanced sedimentation rates along the Veyre delta favoured the collapse of its delta front.

6. Conclusions

A regional limnogeological approach combining sub-lacustrine geomorphology and isotopically dated lacustrine events in the Lakes Tazenat, Chambon, Lacassou and Aydat in the northern part of the French Massif Central provide new evidences for regional landslides impacting river drainage basin (and developing lakes) or lake basin (and eventually developing turbidites). Some similar events are contemporaneous from sedimentary events previously documented in lakes (Pavin, Chauvet, Guéry and Montcineyre) located south of the study area, which suggests regional impact of former palaeo-earthquakes. This result is supported by contemporaneous historical. or early Holocene seis-

mites identified in the Limagne paludal sequence by Vernet (2013). Clusters of regional earthquakes with epicentres located near the Limagne fault (AD 1450–1470; AD 580–650) or beneath the Puy-de-Sancy volcano (AD 1220–1280) are suggested in this study. Clusters of palaeo-earthquakes in AD 580–650 are evidenced by a seismite in the Limagne basin, a MWD2 in Lake Tazenat, and by a slump, a crater outburst flood event and a resulting lake-level drop in Lake Pavin, 55 km south of Tazenat. Clusters of palaeo-earthquakes in AD 1220–1280 are documented by MWDs and sometimes associated turbidites in the Lakes Montcineyre, Chauvet, Pavin and Guéry as well as by the last Dent du Marais Landslide that created lakes Lacassou and Chambon 2 around AD 1215 ± 50. Lake Chambon 2 and Lake Lacassou would therefore be the youngest lakes from the French Massif Central. This cluster was also probably the cause behind a second lake-level fall in Lake Pavin, with a ca. 4.8 m drop associated with an outburst flood and a large subaquatic slide in the deep central basin. Holocene earthquakes near the Limagne fault are also suggested in Lake Tazenat (by MWD3) around 2250 ± 60 cal. BP and around 2730 ± 30 cal. BP (by MWD4), but additional investigations are needed to confirm the seismic origin of MWDs and event-layers recorded in this lake. Radionuclide dating of multiple gravity cores in Lake Tazenat are needed to date MWD1 coeval slope failures and to test the impact of the cluster of major Limagne earthquakes between AD 1450 and 1470 near the Limagne fault. Future investigations in the FMC should also include long coring in maar lakes formed during the last glacial period (Chauvet and Tazenat) and in Lake Chambon to extend the evaluation of natural hazards associated with former earthquakes in the FMC during the Holocene and Late-Glacial period.

Funding

This research and postdoctoral grant to A. F. was supported by the METEOR project (2016–2020) from the AELB (Agence de l'Eau Loire Bretagne) coordinated at Tours University and by the EDIFIS project (2012–2015) from the AELB coordinated at Orleans University.

Declaration of competing interest

The authors declare that they have no known competing financial interests or personal relationships that could have appeared to influence the work reported in this paper.

Acknowledgments

We thank Charles Gumiaux (ISTO Orléans) for his supervision of GIS modeling on Lake Aydat during the master project of Vivien Janvier in 2010. We also warmly thank Dominique Laffly (UT2J, Toulouse) for his contribution to the development of the EDFISegY software together with GeoHyd-ANTEA Group engineers within the frame of the EDIFIS project. This study benefited from fruitful scientific discussions with Etienne Juvigné on Lake Tazenat, and with Yannick Miras and Pierre Boivin on the Lakes Aydat, Pavin and Chambon. LIDAR data from Lake Tazenat and Lake Pavin used in this study were produced by the CRAIG from Clermont-Ferrand within the frame of "Espace Naturel Sensible (ENS) Pavin et Creux de Soucy" and Archeomap programs in 2015 and 2017, respectively. This manuscript was improved by the constructive comments of two anonymous reviewers. We thank Jean Nicolas Haas for coordinating the 41st International Moor Excursion to the Massif Central in 2017, and for editing this special issue.

References

Albéric, P., Jézéquel, D., Bergonzini, L., Chapron, E., Viollier, E., Massault, M., Michard, G., 2013. Carbon cycling and organic radiocarbon reservoir effect in a meromictic crater lake (Lac Pavin, Puy-de-Dôme, France). Radiocarbon 55, 1029–1042.

Allios, D., 2015. Murol, la Forteresse Muette. Presses Universitaires de Rennes, p. 216.

Arnaud, F., Poulenard, J., Giguet-Covex, C., Wilhelm, Revillon, S., Jenny, J.P., Revel, M., Enters, D., Bajard, M., Fouinat, L., Doyen, E., Simonneau, A., Pignol, C., Chapron, E., Vannières, B., Sabatier, P., 2016. Erosion under climate and human pressures: an alpine lake sediment perspective. Quat. Sci. Rev. 152, 1–18.

Arnaud, F., Révillon, S., Debret, M., Revel, M., Chapron, E., Jacob, J., Giguet-Covex, C., Poulenard, J., Magny, M., 2012. Lake Bourget regional erosion patterns reconstruction reveals Holocene NW European Alps soil evolution and paleohydrology. Quat. Sci. Rev. 51, 81–92.

Arricau, V., 2020. Géohistoire des risques naturels de trois lacs du cratère emblématiques du Massif Central français (lacs Pavin, Tazenat et Issarlès) Master 2 GEP report Université Toulouse Jean Jaurès, p. 103.

Auriat, S., 1957. Etude des sondages et captages dans plusieurs coulées de la Chaîne des Puys (Balmet, Côme, Louchadières, Aydat, Tiretaine). Rev. Sci. Nat. d'Auvergnes 23, 97–141.

Beck, C., 2009. Late Quaternary lacustrine paleo-seismic archives in north-western Alps: examples of earthquake-origin assessment of sedimentary disturbances. Earth Sci. Rev. 96, 327–344.

Beck, C., Manalt, F., Chapron, E., van Rensbergen, P., de Batist, M., 1996. Enhanced seismicity in the early post-glacial period: evidence from the post-Würm sediments of Lake Annecy, Northwestern Alps. J. Geodyn. 22, 155–171.

Boivin, P., Besson, J.C., Briot, D., Camus, G., de Gor de Herve, A., Gougaud, A., et al., 2009. Volcanologie de la Chaîne des Puys. Edition du Parc Régional des Volcans d'Auvergne, Aydat, France, p. 196.

Chapron, E., 2016. Eléments de diagnose des sédiments fluviatiles stockés à l'amont des retenues sur cours d'eau avant effacement. Rapport scientifique. Agence de l'Eau Loire-Bretagne, p. 76.

Chapron, E., Albéric, P., Jézequel, D., Versteeg, W., Bourdier, J.L., Sitbon, J., 2010. Multidisciplinary characterisation of sedimentary processes in a recent maar lake (Lake Pavin, French Massif Central) and implication for natural hazards. Nat. Hazards Earth Syst. Sci. 10, 1815–1827.

Chapron, E., Ariztegui, D., Mulsow, S., Villarosa, G., Pino, M., Outes, V., Juviginé, E., Crivelli, E., 2006. Impact of the 1960 major subduction earthquake in Northern Patagonia (Chile, Argentina). Quat. Int. 158, 58–71.

Chapron, E., Beck, C., Pourchet, M., Deconinck, J.F., 1999. 1822 earthquake-triggered homogenite in lake le bourget (NW Alps). Terra. Nova 11, 86–92.

Chapron, E., Chassiot, L., Lajeunesse, P., Ledoux, G., Albéric, P., 2016a. Lake Pavin sedimentary environments. In: Sime-Ngando, T. (Ed.), et al., Lake Pavin History, Geology, Biogeochemistry and Sedimentology of a Deep Meromictic Maar Lake. Springer International Publishing Switzerland, pp. 365–379 (Chapter 22).

Chapron, E., Juvigné, E., Mulsow, S., Ariztegui, D., Magand, O., Bertrand, S., Pino, M., Chapron, O., 2007. Recent clastic sedimentation processes in lake puyehue (Chilean lake district, 40.5°S). Sediment. Geol. 201, 365–385.

Chapron, E., Ledoux, G., Simonneau, A., Albéric, A., St-Onge, G., Lajeunesse, P., Boivin, P., Desmet, M., 2012. New evidence of Holocene mass wasting events in recent volcanic lakes from the French Massif Central (lakes Pavin, Montcineyre and Chauvet) and implications for Natural Hazards. In: Yamada, Y. (Ed.), et al., Submarine Mass Movements and Their Consequences, Advances in Natural and Technological Hazards Research 31. Springer Science + Business Media B.V., pp. 255–264 (Chapter 23).

Chapron, E., Simonneau, A., Ledoux, G., Arnaud, F., Lajeunesse, P., Albéric, P., 2016b. French alpine foreland Holocene paleoseismology revealed by coeval mass wasting deposits in glacial lakes. In: Lamarche, G. (Ed.), et al., Submarine Mass Movements and Their Consequences, Advances in Natural and Technological Hazards Research 41. Springer International Publishing Switzerland, pp. 341–349 (Chapter 34).

Chassiot, L., Chapron, E., Di Giovanni, C., Albéric, P., Lajeunesse, P., Lehours, A.C., Meybeck, M., 2016a. Extreme events in the sedimentary record of maar Lake Pavin: implications for natural hazards assessment in the French Massif Central. Quat. Sci. Rev. 141, 9–25.

Chassiot, L., Chapron, E., Di Giovanni, C., Lajeunesse, P., Tachikawak, K., Garcia, M., Bard, E., 2016b. Historical seismicity of the Mont Dore volcanic province (Auvergne, France) unraveled by a regional lacustrine investigation: new insights about lake sensitivity to earthquakes. Sediment. Geol. 339, 134–150.

Chassiot, L., Chapron, E., Miras, Y., Schwalb, M.J., Albéric, P., Beauger, A., Develle, A.L., Arnaud, F., Lajeunesse, P., Zocatelli, R., Bernard, S., Lehours, A.C., Jézéquel, D., 2016c. Lake Pavin paleolimnology and event stratigraphy. In: Sime-Ngando, T. (Ed.), et al., Lake Pavin History, Geology, Biogeochemistry and Sedimentology of a Deep Meromictic Maar Lake. Springer International Publishing Switzerland, pp. 381–406 Chapter, 23.

Chassiot, L., Miras, Y., Chapron, E., Develle, A.L., Arnaud, F., Motelica-Heino, M., Di Giovanni, C., 2018. A 7000-year environmental history and soil erosion record inferred from the deep sediments of Lake Pavin (Massif Central, France). Palaeogeogr. Palaeoclimatol. Palaeoecol. 497, 218–233.

Chassiot, L., Simonneau, A., Chapron, E., Di Giovanni, C., This Issue. Lacustrine records of last millennium sediment yield in the French Massif Central: anthropogenic vs. natural signals. Quat. Int..

U. Danzeglocke O. Joris B. Weninger CalPal-2007 online http://www.calpal-online.de/ 2011 s5 October 2011

De Crespin de Billy, V., Reyes-Marchant, P., Lair, N., Valadas, B., 2000. Impact of agricultural practices on a small headwater stream: terrestrial and aquatic characteristics and self-purifying processes. Hydrobiologia 421, 129–139.

Defive, E., Raynal, J.-P., Ancrenaz, A., Poiraud, A., 2019. L'englacement quaternaire du Massif central. In: Boivin, P., Mercier, F., Coord (Eds.), Histoire de la découverte géologique du Massif central français. In: Mémoire de la Société d'Histoire Naturelle d'Auvergne no., vol. 8. pp. 145–171.

Delebecque, A., 1898. Les Lacs Français. Typographie Chamerot et Reynaud, Paris, p. 436.

Densmore, A.L., Hetzel, R., Ivy-Ochs, S., Krugh, W.C., Dawers, N., Kubik, P., 2009. Spatial variations in catchment-averaged denudation rates from normal fault footwalls. Geology 37, 1139–1142.

Deplazes, G., Anselmetti, F.S., Hajdas, I., 2007. Lake sediments deposited on the Flims

rockslide mass: the key to date the largest mass movement of the Alps. Terra. Nova 19, 252–258.
Dupuis, A., Bossuet, G., Choquier, A., De Luca, P., Macaire, J.J., 1996. Contribution des méthodes électriques de la géophysique appliquée à l'évaluation des bilans sédimentaires. Exemple du bassin du lac Chambon (Puy-de-Dôme). Géol. France 4, 79–87.
Etlicher, B., de Goër de Herve, A., 1988. Téphrochronologie du Tardiglaciaire et de l'Holocène dans le Cantal, le Cézallier et les Monts Dore (Massif Central, France): résultats nouveaux et synthèse. Bull. Assoc. Fr. Étude Quat. 25, 103–110.
Foucher, A., Evrard, O., Cerdan, O., Chabert, C., Lecompte, F., Lefèvre, I., Vandromme, R., Salvador-Blanes, S., 2019. A quick and low-cost technique to identify layers associated with heavy rainfall in sediment archives during the Anthropocene. Sedimentology 67, 486–501.
Foucher, A., Evrard, O., Huon, S., Curie, F., Lefèvre, I., Vaury, V., Cerdan, O., Vandromme, R., Salvador-Blanes, S., 2020. Regional trends in eutrophication across the Loire river basin during the 20th century based on multi-proxy paleolimnological reconstructions. Agric. Ecosyst. Environ. 301, 107065.
Gay, I., 1995. Evolution des flux minéraux pendant le Tardiglaciaire et l'Holocène dans un bassin montagneux à roches magmatiques sous latitude moyenne. Le bassin du lac Chambon, Massif Central, France PhD thesis Université d'Orléans, p. 208.
Gay, I., Macaire, J.J., 1999. Estimation des taux d'érosion chimique tardiglaciaires et holocènes par la méthode des bilans d'altération. Application au bassin du lac Chambon (Massif central, France). C. R. Acad. Sci. Paris, Sci. terre et des planètes/Earth Planet. Sci. 328, 387–992.
Girardclos, S., Schmidt, O.T., Sturm, M., Ariztegui, D., Anselmetti, F.S., 2007. The 1996 AD delta collapse and large turbidite in Lake Brienz. Mar. Geol. 241, 137–154.
Gomez, B., Corral, A., Orpin, A.R., Page, M.J., Pouderoux, H., Upton, P., 2015. Lake Tutira paleoseismic record confirms random, moderate to major and/or great Hawke's Bay (New Zealand) earthquakes. Geology 43, 103–106.
Gratuze, B., Blet-Lemarquand, M., Barrandon, J.N., 2001. Mass spectrometry with laser sampling: a new tool to characterize archaeological materials. J. Radioanal. Nucl. Chem. 247, 645–656.
Hansen, L., Waldmann, N., Storms, J.E.A., Eilertsen, R.S., Ariztegui, D., Chapron, E., Nesje, A., 2016. Morphological signatures of mass wasting and delta processes in a fjord-lake system: insights from Lovatnet, western Norway. Norw. J. Geol. 96, 1–21.
Hovius, N., Meunier, P., Ching-Weei, L., Hongey, C., Yue-Gau, C., Dadson, S., Horng, M.-J., Lines, M., 2011. Prolonged seismically induced erosion and the mass balance of a large earthquake. Earth Planet Sci. Lett. 304, 347–355.
Howarth, J., Fitzsimons, S.J., Norris, R.J., Jacobsen, G.E., 2013. Lake sediments record cycles of sediment flux driven by large earthquakes on the Alpine fault, New Zealand. Geology 40, 1091–1094.
Jouannic, G., Walter-Simonnet, A.V., Bossuet, G., Cubizolle, H., Boivin, P., Devidal, J.L., Oberlin, C., 2014. Occurrence of an unknown Atlantic eruption in the Chaîne des Puys volcanic field (Massif Central, France). J. Volcanol. Geoth. Res. 283, 94–100.
Juvigné, E., Miallier, D., 2016. Distribution, tephrostratigraphy and chronostratigraphy of the widespread eruptive products of Pavin Volcano. In: Sime-Ngando, T. (Ed.), et al., Lake Pavin History, Geology, Biogeochemistry and Sedimentology of a Deep Meromictic Maar Lake. Springer International Publishing Switzerland, pp. 143–154 (Chapter 8).
Juvigné, E., Stach-Czerniak, A., 1998. Etude sédimentologique et playnologique des dépôts lacustres tardiglaciaires et holocènes du Gour de Tazenat (Massif Central, France). Quaternaire 9, 15–23.
Knapp, S., Gilli, A., Anselmetti, F.S., Krautblatter, M., Hajdas, I., 2017. Multistage rock-slope failures revealed in lake sediments in a seismically active alpine region (Lake Oeschinen, Switzerland). J. Geophys. Res.: Earth Surf. 123, 658–677.
Kremer, K., Corella, J.P., Adatte, T., Garnier, E., Zenhäusern, G., Girdardclos, S., 2015. Origin of turbidites in deep Lake Geneva (France-Switzerland) in the last 1500 years. J. Sediment. Res. 85, 1455–1465.
Labuhn, I., Hammarlund, D., Chapron, E., Czymzik, M., Dumoulin, J.P., Nilson, A., Régnier, E., Robygd, J., von Grafenstein, U., 2018. Holocene hydroclimate variability in Central Scandinavia inferred from flood layers in contourite drift deposits in Lake Storsjön. Quaternary 1, 1–24.
Lauterbach, S., Chapron, E., Brauer, A., Hüls, M., Gilli, A., Arnaud, F., Piccin, A., Nomade, J., Desmet, M., von Grafenstein, U., Participants, D., 2012. A sedimentary record of Holocene surface runoff events and earthquake activity from Lake Iseo (Southern Alps, Italy). Holocene 22, 749–760.
Lavrieux, M., Disnar, J.R., Chapron, E., Bréheret, J.G., Jacob, J., Miras, Y., Reyss, J.L., Andrieu-Ponel, V., Arnaud, F., 2013a. 6700 yr sedimentary record of climatic and anthropogenic signals in Lake Aydat (French Massif Central). Holocene 23, 1317–1328.
Lavrieux, M., Jacob, J., Disnar, J.R., Bréheret, J.G., Le Milbeau, C., Miras, Y., Andrieu-Ponel, V., 2013b. Sedimentary cannabinol tracks the history of hemp retting. Geology 41, 751–754.
Lavrieux, M., Jacob, J., Le Milbeau, C., Zocatelli, R., Masuda, K., Bréheret, J.G., Disnar, J. R., 2011. Occurrence of triterpenyl acetates in soil and their potential as chemotaxonomical markers of Asteracaea. Org. Geochem. 42, 1315–1323.
Legrand, B., Miras, Y., Beauger, A., Dussauze, M., Latour, D., 2019. Akinetes and ancient DNA reveal toxic cyanobacterial recurrences and their potential for resurrection in a 6700-year-old core from a eutrophic lake. Sci. Total Environ. 687, 1369–1380.
Macaire, J.J., Bossuet, G., Choquier, A., Cocirta, C., de Luca, P., Dupuis, A., Gay, I., Mathey, E., Guenet, P., 1997. Sediment yield during late glacial and Holocene periods in the lac Chambon watershed, massif central, France. Earth Surf. Process. Landforms 22, 473–489.
Macaire, J.J., Cocirta, C., De Luca, P., Gay, I., Goer de Herve, A., 1992. Origines, âges et évolution des systemes lacustres tardi- et postglaciaires dans le bassin du lac Chambon (Puy-de-Dôme, France), C.R.. Acad. Sci. Paris 315, 1119–1125.
Magny, M., Combourrieu-Nebout, N., de Beaulieu, J.L., Bout-Roumazeilles, V., Colombaroli, D., Desprat, S., Francke, A., Joannin, S., Ortu, E., Peyron, O., Revel, M., Sadori, L., Siani, G., Sicre, M.A., Samartin, S., Simonneau, A., Tinner, W., Vannière, B., Wagner, B., Zanchetta, G., Anselmetti, F., Brugiapaglia, E., Chapron, E., Debret, M., Desmet, M., Didier, J., Essallami, L., Galop, D., Gilli, A., Haas, J.N., Kallel, N., Millet, L., Stock, A., Turon, J.L., Wirth, S., 2013. North-South palaeohydrological contrasts in the central Mediterranean during the Holocene: tentative synthesis and working hypotheses. Clim. Past 9, 2043–2071.
Mallet, J.P., Restituto, F., Leitao, M., Henry, C., Bernoud, S., Laffont, M., Richeux, C., Henry, C., Verges, C., 2006. Programme 2005 de caractérisation et de suivi de masses d'eau de plan d'eau. Agence de l'Eau Loire-Bretagne, Rapport final, p. 243.
Meyers, P., 1994. Preservation of elemental and isotopic source identification of sedimentary organic matter. Chem. Geol. 114, 289–302.
Miallier, D., 2020. Variations récents de niveau du lac Pavin: essai de mise en cohérence des différentes sources d'information. BSGF-Earth Sci. Bull. 191, 4–21.
Miallier, D., Boivin, P., Pilleyre, T., Choupin, L., Malterre, D., Sanzelles, S., 2008. Les téphras du Pariou (chaîne des Puys, France): nouvelles observations sur la dispersion proximale, apports téphrostratigraphiques. Quaternaire 19, 87–96.
Miras, Y., Beauger, A., Lavrieux, M., Berthon, V., Serieyssol, K., Andrieu-Ponel, V., Ledgeret, P.M., 2015. Tracking long-term human impacts on landscape, vegetal biodiversity and water quality in the Lake Aydat catchment (Auvergne, France) using pollen, non-pollen palynomorphs and diatom assemblages. Palaeogeogr. Palaeoclimatol. Palaeoecol. 424, 76–90.
Miras, Y., Laggoun-Défarge, F., Guenet, P., Richard, H., 2004. Multi-disciplinary approach to changes in agro-pastoral activities since the Sub-Boreal in the surroundings of the "narse d'Espinasse" (Puy de Dôme, French Massif Central). Veg. Hist. Archaeobotany 13, 91–103.
Moernaut, J., Verschuren, D., Charlet, F., Kristen, I., Fagot, M., De Batist, M., 2010. The seismic-stratigraphic record of lake-level fluctuations in Lake Challa: hydrological study and change in equatorial East Africa over the last 140 kyr. Earth Planet Sci. Lett. 290, 214–223.
Mulder, T., Chapron, E., 2011. Flood deposits in continental and marine environments: character and significance. In: Slatt, R.M., Zavala, C. (Eds.), Sediment Transfer from Shelf to Deep Water – Revisiting the Delivery System: AAPG Studies in Geology, vol. 61. pp. 1–30.
Mulder, T., Cochonat, P., 1996. Classification of offshore mass movements. J. Sediment. Geol. 66, 43–57.
Nepop, R., Agatova, A., 2016. Quantitative estimations of the Holocene erosion due to seismically induced landslides in the SE Altai (Russia) applying detailed profiling and statistical approaches. Int. J. Geohazards Environ. 2, 104–118.
Normandeau, A., Lajeunesse, P., Philibert, G., 2013. Late-Quaternary morphostratigraphy of Lake St-Joseph (southeastern Canadian Shield): evolution from a semi-enclosed glacimarine basin to a postglacial lake. Sediment. Geol. 295, 38–52.
Oswald, P., Strasser, M., Hammerl, C., Moernaut, J., 2021. Seismic control of large prehistoric rockslides in the Eastern Alps. Nat. Commun. 12 article number1059.
Pollet, N., Cojean, R., Couture, R., Schneider, J.L., Strom, A.L., Voirin, C., Wassmer, P., 2005. A slab-on-slab model for the Flims rockslide (Swiss Alps). Can. Geotech. J. 42, 587–600.
Pollet, N., Schneider, J.L., 2004. Dynamic disintegration processes accompanying transport of the Holocene Flims sturzstrom (Swiss Alps). Earth Planet Sci. Lett. 221, 433–448.
Rapuc, W., Sabatier, P., Andric, M., Crouzet, C., Arnaud, F., Chapron, E., Smuc, A., Develle, A.L., Wilhelm, B., Demory, F., Reyss, J.L., Régnier, E., Daut, G., von Grafenstein, U., 2018. 6600 years of earthquake record in the julian Alps (lake bohinj, Slovenia). Sedimentology 65, 1777–1799.
Ross, K.A., Schmid, M., Ogorka, S., Muvundja, F.A., Anselmetti, F.S., 2015. The history of subaquatic volcanism record in the sediments of Lake Kivu, East Africa. J. Paleolimnol. 54, 137–152.
Schneider, J.L., Pollet, N., Chapron, E., Wessels, M., Wassmer, P., 2004. Signature of Rhine valley sturzstrom dam failures in Holocene sediments of Lake Constance, Germany. Sediment. Geol. 169, 75–91.
Schneider, C.A., Rasband, W.S., Eliceiri, K.W., 2012. NIH Image to ImageJ: 25 years of image analysis. Nat. Methods 9, 671–675.
Simonneau, A., Chapron, E., Courp, T., Tachikawa, K., Le Roux, G., Baron, S., Galop, D., Garcia, M., Di Giovanni, C., Motellica-Heino, M., Mazier, F., Foucher, A., Houet, T., Desmet, M., Bard, E., 2013a. Recent climatic and anthropogenic imprints on lacustrine systems in the Pyrenean Mountains inferred from minerogenic and organic clastic supply (Vicdessos valley, Pyrenees, France). Holocene 23, 1764–1777.
Simonneau, A., Chapron, E., Vannière, B., Wirth, S.B., Gilli, A., Di Giovanni, C., Anselmetti, F.S., Desmet, M., Magny, M., 2013b. Mass-movement and flood-induced deposits in Lake Ledro, Southern Alps, Italy: implications for Holocene palaeohydrology and natural hazards. Clim. Past 9, 1–16.
Sims, J.D., 2012. Earthquake-induced load casts, pseudonodules, ball-and-pillow structures, and convolute lamination: additional deformation structures for paleoseismic studies. In: Cox (Ed.), et al., Recent Advances in North American Paleoseismology and Neotectonics East of the Rockies. In: Geological Societey of America Special Paper, vol. 493. pp. 191–201.
Stebich, M., Bruchmann, C., Kulbe, T., Negendank, J.F.W., 2005. Vegetation history, human impact and climate change during the last 700 years recorded in annually laminated sediments of Lac Pavin, France. Rev. Palaeobot. Palynol. 133, 115–133.
Strasser, M., Monecke, K., Schnellmann, M., Anselmetti, F.S., 2013. Lake sediments as natural seismographs: a compiled record of Late Quaternary earthquakes in Central Switzerland and its implication for Alpine deformation. Sedimentology 60, 319–341.
Thouret, J.C., Boivin, P., Labazuy, P., Leclerc, A., 2016. Geology, geomorphology and slope instability of the maar lake Pavin (Auvergne, French Massif Central). In: Sime-Ngando, T. (Ed.), et al., Lake Pavin History, Geology, Biogeochemistry and Sedimentology of a Deep Meromictic Maar Lake. pp. 155–174 (Chapter 9).
Valentine, G.A., Briner, J.P., van Wyk de Vries, B., Macorps, E., Gump, D., 2019. ^{10}Be

exposure ages for the Late Pleistocene Gour de Tazenat (Chaîne des Puys volcanic filed, Auvergne, France). Quat. Geochronol. 50, 8–13.
Van Daele, M., Moernaut, J., Doom, L., Boes, E., Fontijn, K., Heirman, K., Vandoorne, W., Hebbeln, D., Pino, M., Urrutia, R., Brummer, R., De Batist, M., 2015. A comparison of the sedimentary records of the 1960 and 2010 great Chilean earthquakes in 17 lakes: implications for quantitative lacustrine palaeoseismology. Sedimentology 62, 1466–1496.
Vernet, G., 2013. La séquence sédimentaire des Gravanches/Gerzat: enregistrement d'événements «catastrophiques» à valeur chronologiques en Limagne d'Auvergne (Massif Central, France). Quaternaire 24, 109–127.
Vidal, N., de Goër de Herve, A., Camus, G., 1996. Déstabilisation de reliefs d'érosion en terrain volcanique. Exemples pris dans le Massif Central Français. Quaternaire 7, 117–127.
Wirth, S., Gilli, A., Simonneau, A., Ariztegui, D., Vannière, B., Glur, L., Chapron, E., Magny, M., Anselmetti, F.S., 2013. A 2000 year-long seasonal record of floods in the southern European Alps. Geophys. Res. Lett. 40, 4025–4029.